Athens Journal of Technology & Engineering

Athens Journal of Technology & Engineering

Published by the Athens Institute for Education and Research (ATINER)

****
*

ATINER is an Athens-based World Association of Academics and Researchers based in Athens. ATINER is an independent and non-profit Association with a Mission to become a forum where Academics and Researchers from all over the world can meet in Athens, exchange ideas on their research and discuss future developments in their disciplines, as well as engage with professionals from other fields. Athens was chosen because of its long history of academic gatherings, which go back thousands of years to Plato's Academy and Aristotle's Lyceum. Both these historic places are within walking distance from ATINER's downtown offices. Since antiquity, Athens was an open city. In the words of Pericles, Athens"…is open to the world, we never expel a foreigner from learning or seeing". ("Pericles' Funeral Oration", in Thucydides, The History of the Peloponnesian War). It is ATINER's mission to revive the glory of Ancient Athens by inviting the World Academic Community to the city, to learn from each other in an environment of freedom and respect for other people's opinions and beliefs. After all, the free expression of one's opinion formed the basis for the development of democracy, and Athens was its cradle. As it turned out, the Golden Age of Athens was in fact, the Golden Age of the Western Civilization. Education and (Re)searching for the 'truth' are the pillars of any free (democratic) society. This is the reason why Education and Research are the two core words in ATINER's name.
****

The **Athens Journal of Technology & Engineering (AJTE)** is an Open Access quarterly double-blind peer reviewed journal and considers papers from all areas engineering (civil, electrical, mechanical, industrial, computer, transportation etc), technology, innovation, new methods of production and management, and industrial organization. Many of the papers published in this journal have been presented at the various conferences sponsored by the Engineering & Architecture Division of the Athens Institute for Education and Research (ATINER). All papers are subject to ATINER's Publication Ethical Policy and Statement.

Athens Journal of Technology & Engineering
Editorial and Reviewers' Board

President's Message

All ATINER's publications including its e-journals are open access without any costs (submission, processing, publishing, open access paid by authors, open access paid by readers etc.) and is independent of presentations at any of the many small events (conferences, symposiums, forums, colloquiums, courses, roundtable discussions) organized by ATINER throughout the year and entail significant costs of participating. The intellectual property rights of the submitting papers remain with the author. Before you submit, please make sure your paper meets the basic academic standards, which includes proper English. Some articles will be selected from the numerous papers that have been presented at the various annual international academic conferences organized by the different divisions and units of the Athens Institute for Education and Research. The plethora of papers presented every year will enable the editorial board of each journal to select the best, and in so doing produce a top-quality academic journal. In addition to papers presented, ATINER will encourage the independent submission of papers to be evaluated for publication.

The current issue is the fourth of the eleventh volume of the *Athens Journal of Technology & Engineering (AJTE)*, published by the Engineering & Architecture Division of ATINER.

Gregory T. Papanikos, President, ATINER.

Athens Institute for Education and Research
A World Association of Academics and Researchers

15th Annual International Conference on Civil Engineering
23-26 June 2025, Athens, Greece

The Civil Engineering Unit of ATINER is organizing its **15th Annual International Conference on Civil Engineering, 23-26 June 2025, Athens, Greece** sponsored by the Athens Journal of Technology & Engineering. The aim of the conference is to bring together academics and researchers of all areas of Civil Engineering other related areas. You may participate as stream leader, presenter of one paper, chair of a session or observer. Please submit a proposal using the form available (https://www.atiner.gr/2025/FORM-CIV.doc).

Academic Members Responsible for the Conference

- **Dr. Dimitrios Goulias**, Head, Civil Engineering Unit, ATINER and Associate Professor & Director of Undergraduate Studies Civil & Environmental Engineering Department, University of Maryland, USA.

Important Dates
- Abstract Submission: **3 March 2025**
- Acceptance of Abstract: 4 Weeks after Submission
- Submission of Paper: **26 May 2025**

Social and Educational Program
The Social Program Emphasizes the Educational Aspect of the Academic Meetings of Atiner.
- Greek Night Entertainment (This is the official dinner of the conference)
- Athens Sightseeing: Old and New-An Educational Urban Walk
- Social Dinner
- Mycenae Visit
- Exploration of the Aegean Islands
- Delphi Visit
- Ancient Corinth and Cape Sounion

Conference Fees

Conference fees vary from 400€ to 2000€
Details can be found at: https://www.atiner.gr/fees

Athens Institute for Education and Research
A World Association of Academics and Researchers

13th Annual International Conference on Industrial, Systems and Design Engineering, 23-26 June 2025, Athens, Greece

The [Industrial Engineering Unit](#) of ATINER will hold its **13th Annual International Conference on Industrial, Systems and Design Engineering, 23-26 June 2025, Athens, Greece** sponsored by the [Athens Journal of Technology & Engineering](#).The aim of the conference is to bring together academics, researchers and professionals in areas of Industrial, Systems, Design Engineering and related subjects. You may participate as stream leader, presenter of one paper, chair of a session or observer. Please submit a proposal using the form available (https://www.atiner.gr/2025/FORM-IND.doc).

Important Dates
- Abstract Submission: **3 March 2025**
- Acceptance of Abstract: 4 Weeks after Submission
- Submission of Paper: **26 May 2024**

Academic Member Responsible for the Conference

- **Dr. Theodore Trafalis**, Director, [Engineering & Architecture Division](#), ATINER, Professor of Industrial & Systems Engineering and Director, Optimization & Intelligent Systems Laboratory, The University of Oklahoma, USA.

Social and Educational Program
The Social Program Emphasizes the Educational Aspect of the Academic Meetings of Atiner.
- Greek Night Entertainment (This is the official dinner of the conference)
- Athens Sightseeing: Old and New-An Educational Urban Walk
- Social Dinner
- Mycenae Visit
- Exploration of the Aegean Islands
- Delphi Visit
- Ancient Corinth and Cape Sounion
    More information can be found here: https://www.atiner.gr/social-program

---

Conference Fees
Conference fees vary from 400€ to 2000€
Details can be found at: https://www.atiner.gr/fees

Composite Command Pattern for Managing Spherical Geometry Constructions

By Hans Dulimarta[*] & William Dickinson[±]

Spherical Easel (https://easelgeo.app) is a free web application for researching, teaching, and learning spherical geometry written in Typescript. The authors have created an open-source code base in VueJS v3 that combines several design patterns, global data structures, and cloud-based storage for storing and retrieving spherical constructions. Spherical constructions are made up of interdependent geometric objects (like lines and circles). Interdependencies means that while being moved, updates to a single object must propagate to other dependent objects. The application stores the dependency structure using a directed acyclic graph to allow these updates to propagate correctly. In this paper, we describe how Spherical Easel employs the Command and Composite design patterns (fully integrated with various VueJS supporting libraries) to maintain a history of construction edits, allowing users to undo and redo edits, and to store a final construction script in a cloud database. To guarantee correct rendering of the spherical objects when loading a construction, the stored script also preserves the structure of the directed acyclic graph. The construction script parser built is also designed to take advantage of the (Composite) Command design pattern. Using this innovative design, adding new object types does not require a major redesign of the script parser.

Keywords: *Spherical geometry, software design patterns, web application*

Introduction

Spherical geometry is the earth's geometry, surrounds us all, and is obviously important for many large-scale applications. For example, spherical lines, like the equator and longitudes (but not latitudes), are the paths that orbiting satellites' earthly shadows follow. Despite its obvious applied nature, spherical geometry is rarely taught at the secondary level in the United States. This contrasts with Euclidean geometry, which is always taught at the secondary level. Changing this is one of the goals of our spherical geometry modeling application; one ultimate ideal use of Spherical Easel would be to have students at all levels (secondary and beyond) and in all countries be exposed to spherical geometry using this app whenever they are taught Euclidean geometry.

To effectively learn about, teach, and conduct research in spherical geometry, students, teachers, and researchers must be able to easily interact with and explore it. While Euclidean geometry is easily modeled on paper or a white board, spherical geometry is more challenging to physically model. Tennis balls are a cheap but ineffective option and Lénárt Spheres (large clear plastic spheres one

[*]Professor, School of Computing, Grand Valley State University, USA.
[±]Professor, Department of Mathematics, Grand Valley State University, USA.

can draw on) are expensive. This leaves dynamic digital tools for such explorations. While there are multiple digital tools for exploring Euclidean geometry including GeoGebra and Desmos and a few tools for exploring hyperbolic geometry like NonEuclid, *Spherical Easel is the only dedicated free tool for dynamically modeling spherical (or double elliptic) geometry that is currently available.*

Design Patterns

Software developers who employ the object-oriented paradigm in their development are very likely to have read the *de facto* standard design pattern book by Gamma et al. (1995). The book includes a catalogue of 23 commonly used design patterns in object-oriented programming. Since then, many other books/resources have been published, and the catalog items have been greatly expanded. For example, some of them are specific to a particular language (Smalltalk (Back 1997), Java Design Patterns), others are targeted for specific programming modes (concurrent programming (Schmidt et al. 2000), reactive programming (Oliveira Marum et al. 2024)), and others are specific to an application domain (game programming (Nystrom 2014), block chain smart contracts (Górski 2024)).

The focus of this paper is an extensive exposition of how the Command and Composite design patterns are incorporated into Spherical Easel. In Gamma et al. (1995) the intent of each design pattern is given as:

> **Command**: *encapsulate a request as an object*, thereby letting you parameterize clients with different requests, queue, or log requests, and *support undoable operations*.
> **Composite:** compose objects into tree structures to represent part-whole hierarchy. Composite lets *clients treat individual objects and compositions of objects uniformly*.

The *italics* in each quote indicate the part of each pattern that Spherical Easel uses extensively and will be the focus of this paper.

Spherical Easel

Spherical Easel is a web-based application offering an abundant suite of tools which enable users to create constructions of spherical objects including points, lines, segments, circles[1], ellipses and parametric curves. Intersection points between these objects are automatically created and dynamically updated as a user moves construction elements. Users can also transform the geometric objects using spherical rotations, translations, reflections, and inversions. In addition, there are

---

[1]Spherical circles are the intersection of a sphere with a plane. When that plane contains the center of the sphere, a spherical line or great circle or geodesic is formed, like the equator and longitudes on the Earth. Spherical lines are locally paths of shortest distance. When the plane does not contain the center of the sphere, a small circle is formed, like latitudes on the Earth.

tools for constructing tangents, antipodal points, perpendiculars, bisections, and polar lines among many others.

As of summer 2024, Spherical Easel provides 32 tools, grouped under the following eight categories:

Display Tools: Show/Hide Labels, Show/Hide Objects, Zoom in/out/fit, Rotate Sphere, and Move Objects
Basic Tools: Create Lines, Line Segments, Points, and Circles
Construction Tools: Polar, Antipodal, Midpoint, Angle Bisectors, Tangent Lines, Intersections, Perpendicular Lines, and Points on Objects
Measurement Tools: Coordinates, Angle, Triangle Area, and Polygon Area
Measured Objects: Measured Circle
Advanced Tools: Three Point Circle, N-sect Segments, and N-sect Angle
Conic Tool: Create Ellipse
Transformation Tools: Reflection, Point Reflection, Rotation, Inversion, Translation, and Apply Transformation

Figure 1. *The Main Page of Spherical Easel at https://easelgeo.app Showing a Circle and Two Lines Tangent to the Circle*
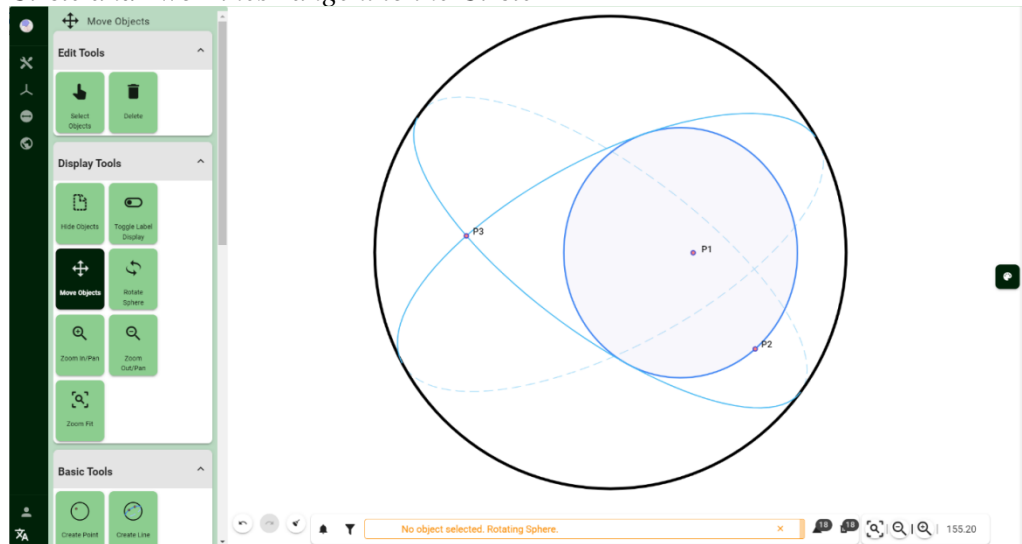
In addition, it provides a calculation facility for computing mathematical functions of measured objects (like area, length, distance, or angles) and a limited functionality for plotting and interacting with simple spherical parametric curves. To the best of our knowledge, Spherical Easel is the first web-based application for **spherical geometry computations** that offers such extensive tools. We plan to implement a suite of about 55 tools; The goal is to implement the analog of any tool found in the digital Euclidean applications previously mentioned or any idea that is mentioned in the historical texts (such as Todhunter (1859)) used during the late 19th century heyday of spherical geometry, like radical axis and centers of similitude.

Among the main problems we attempt to solve in managing spherical constructions are:

- Enabling the user to redo and undo (graphical) edits on the canvas. These user actions must be synchronized with updating the directed acyclic graph (DAG).
- Generating a script that reflects the sequence of object constructions performed by the user on the graphical canvas in a format which can be saved on persistent storage.
- Reloading and interpreting construction scripts from persistent storage and rebuilding the DAG.

Application Architecture and Design Patterns

A more elaborate description of the application architecture and various design patterns used in our application can be found in Dulimarta and Dickinson (2023). In this paper, we focus on the two design patterns which are heavily used in managing saved spherical constructions: the Command and the Composite design patterns.

Directed Acyclic Graph

Spherical objects may be constructed with one or more dependencies. For instance:

A circle created from a center point and a point on its perimeter is dependent on the two points.
Each intersection point between two circles depends on the two circles.
A line might depend on the intersection points of two circles.

Our application stores the dependencies using an important data structure: a directed acyclic graph (DAG) of spherical objects. In the DAG, all the dependencies are stored as parent/child relationships. In Figure 2

Figure 2, the relationships are recorded in two separate arrays: `_parents` and `_kids`.

Figure 2. *SENodule Abstract Class*

```
abstract class SENodule {
  protected _parents: SENodule[] =
[]
  protected _kids: SENodule[] = []
  protected _outOfDate = false

  public abstract update();

  public canUpdateNow(): boolean {
    return !_parents.some(item =>
       item.isOutOfDate()
    )
  }

  public updateKids() {
    const updateNow: number[] = []
    _kids.forEach((item,index) =>
      if (item.canUpdateNow())
        updateNow.push(index))
    updateNow.forEach((kid:number)
=> {
      this._kids[kid].update()
    })
  }

  public addKid(n: SENodule) {
      this._kids.push(n)
  }


  public addParent(n:SENodule) {
      this._parents.push(n)
  }

  public
registerChild(n:SENodule) {
      this.addKid(n);
      n.addParent(this);
  }
}
```

For instance, when creating a circle C between with a center point *P* and point on the perimeter *Q*, the circle C becomes the child of both *P* and *Q*, and *P* (and *Q*) becomes the parent of C. Moving one of the points (*P* or *Q*) to a new position will update the details of circle C. If later the user creates a line *L* through *P* and *Q*, and its intersection *X* with the circle *C*, moving either *P* or *Q* to a new position will also update the position of the intersection point. A snapshot of the DAG representing this construction is shown in Figure 3.

Figure 3. *Directed Acyclic Graph*
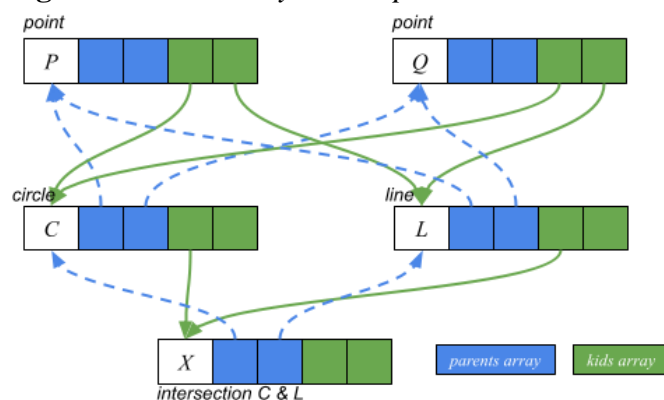
Independent objects (such as *P* and *Q* at the top of the diagram) become root nodes who have no parental dependencies on other objects. These top-level objects can be directly manipulated by users. In a typical construction, we will find a

forest of DAGs each associated with a distinct root node or nodes. In general, any updates to a single object which is also a parent of other objects will propagate to the children, grandchildren, grand-grandchildren, and so on. Before updating a particular object in the DAG, we must check to make sure that all its parents have been updated.

The internal structure of the DAG is implied in the design of the parent abstract class `SENodule` inherited by all the other geometric object classes. The methods `addKid`, `addParent`, and `registerChild` allow the creation of the DAG and before updating a particular object in the DAG, the variable `_outOfDate` is checked and updated with the method `canUpdateNow`. For example, in Figure 3, updates to *X* can be performed only after *L* and *C* are updated. The `updateKids` method allows changes to propagate to the rest of the DAG.

The method that performs the **actual update** is abstract because sometimes the information needed to update an object is not contained in the parent objects. For example, when a line segment connects a pair of antipodal points (like a longitude connecting the north and south poles) the line segment is not uniquely determined by the endpoints, and the update of that line segment depends on a normal vector which is independent of the parent antipodal points. Also, to properly undo a user's action certain pieces of information (like a line segment's normal vector) must be stored and passed along during update propagation.

Handling user Interactions

Users create spherical objects by first selecting one of the tools pictured in the lefthand side of Figure 1. When a selected tool becomes active, Spherical Easel switches to a specific mode associated with that tool. Operating under this mode, user actions to create spherical objects are mapped as a specific Command object or a group of Command objects.

The Command Pattern

Each user action of editing the graphical canvas (creating a new object or modifying/removing an existing object) is recorded as a Command object. When a new object is created, we know that all the objects it depends on and their dependencies must have been already created. We take advantage of this obvious fact by recording the sequence of user actions in a list of commands. Those objects created expand the DAG with new nodes and dependencies. Using the example of creating a circle C with center point *P* and perimeter point *Q* translates to the following three simple commands:

- Create a new point *P* (with no dependencies).
- Create a new point *Q* (with no dependencies).
- Create a new circle C with *P* and *Q* as its parent.

In the command history the above three commands are recorded in the order shown, and the third command unifies the two independent DAGs (each

consisting of a single point) into one DAG. Our implementation of the Command pattern revolves around the following abstract class shown in Figure 4.

Figure 4. *Executable Command*

```
static CMD_HISTORY: Command[] = [];

abstract class Command {
    abstract restoreState(): void;
    abstract saveState(): void;
    abstract do(): void;

    execute(): void {
        CMD_HISTORY.push(this);
        this.saveState();
        this.do();
    }
}
```

Using the Command pattern makes it easy to support undoing (and redoing) of user actions. The `saveState()` call facilitates storing any necessary information that may be needed to restore the data structure when this particular command is being undone. By pushing every executed command to a stack (CMD_HISTORY), undoing user actions can be implemented as a static method that pops the most recent command and invoking its `restoreState()` function as shown in Figure 5.

```
abstract class Command {
    static undo(): void {
        if (CMD_HISTORY.length === 0)
            return;
        const lastAction: Command | undefined = CMD_HISTORY.pop();
        if (lastAction)
            lastAction.restoreState();
```

Figure 5. *Command Undo*

Practically, the `restoreState()` function performs the opposite of the `do()` function and also *in reverse order*. For instance, if the user wants to add a circle C (with label L_c) that depends on existing points P (center) and Q (on the perimeter), in the implementation of `AddCircleCommand`, the sequence of operation of its `do()` and `restoreState()` are shown in Table 1.

Table 1. *Sequence of Operation in AddSegmentCommand*

do()	restoreState()
1. Add *C* as a child of *P* Add *C* as a child of *Q* Add label L_c as a child of *C* Add circle *C* to the list of circle objects Add label L_c to the list of label objects	1. Remove label L_c from the list of label objects Remove circle *C* from the list of circle objects Remove L_c from the children of *C* Remove *S* from the children of *Q* Remove *S* from the children of *P*

It is important to note that the user action of removing an existing object from the graphical canvas is also recorded as a command object. As a result, the graphical canvas may show fewer objects, but the command history will continue to grow longer.

Composite Pattern

For convenience, our graphical editor allows the user to create objects in several ways. For instance, to create a circle *C* as shown in the previous example, the user can perform one of the following actions with using the Point Tool and Circle Tool or both just the Circle Tool:

> Initiate three separate actions: With the Point Tool, first create the first point *P*, then create the second point *Q*. Then with the Circle Tool create a circle with center *P* and containing *Q* by clicking on *P* and dragging to release on *Q* or
> Using only the Circle Tool, in a single action drag and release the mouse from the location of the points (without creating them first).

Although the final visual outcome for both methods is the same, to remove the circle and two points from the canvas the first method requires three calls to `undo()`, while the second method requires only one. To support these features correctly, we apply the Composite design pattern shown in Figure 6.

Figure 6. *Command Group*

```
class CommandGroup extends Command {
    public subCommands: Command[] = [];
     addCommand(c: Command): Command {
        this.subCommands.push(c);
        return this;
    }
    restoreState(): void {
        // Restore state should be done in REVERSE order
        for (let kIdx = subCommands.length - 1; kIdx >= 0; kIdx--) {
            this.subCommands[kIdx].restoreState();
        }
    }
    saveState(): void {
        this.subCommands.forEach(x => { x.saveState() });
    }
    do(): void {
        this.subCommands.forEach(x => { x.do() });
    }
}
```

Using the above definition of `CommandGroup`, creating a circle from two points can be implemented using code snippet as shown in Figure 7.

Figure 7. *Creating a Circle from Two Points*

```
const circleGroup = new CommandGroup();
const createCenter = new AddPointCommand(/*args*/);
const createPeripheral = new AddPointCommand(/*args*/)
const createCircle = new AddCircleCommand(/*args*/);
circleGroup.addCommand(createCenter);
circleGroup.addCommand(createPeripheral);
circleGroup.addCommand(createCircle);
circleGroup.execute();
```

Cloud Database

To provide persistent storage, authenticated users of Spherical Easel are given access to a cloud database for storing their geometric constructions. Specifically, Spherical Easel keeps the user data on the Google Firebase Firestore which stores two different kinds of user data:

- Most user data (user profile, constructions details) which can be encoded as "text format" is stored on Firebase Firestore.
- Binary data related to the constructions (such as construction preview images, compressed textual data) are stored in Firebase Storage.

Incorporating the Firebase Cloud data store into Spherical Easel allows its users to easily share their work with other users. These features, for instance, allow a teacher to prepare several geometric constructions that can be easily shared and built upon by their students or a researcher can easily share and build on a spherical construction.

Generating Geometric Construction Scripts

```
abstract class Command {
    abstract toOpcode(): null | string | Array<string>

    static dumpOpcode(): string {
        const out = CMD_HISTORY.map(c => c.toOpcode())
            .filter(z => z !== null)
        return JSON.stringify(out)
    }
}
```

The Command history data structure, along with the Command Pattern used in Spherical Easel, enables the app to save geometric constructions in the cloud database as a textual script in JSON (JavaScript Object Notation). Every `Command` subclass implements a method to dump its execution context.

Invoking `dumpOpcode()` will iterate over the current sequence of command objects and each command will produce its own JSON representation of its executable context via its implementation of the `toOpcode()` method. For flexibility, this method has multiple return types:

`null`: when the command does not actually create/delete spherical objects, but instead it mainly modifies the visual property of spherical objects on the canvas. For instance, moving the position of a label, changing the visibility of spherical objects, changing the display style of labels fall under this category. Commands under this category do not have to be saved to the cloud database, hence they are filtered out from being converted to the final JSON string.

A single string: when the command executes as a standalone, and not part of a group.

An array of strings: when several related commands must execute as a group.

Since the implementation of `opCode()` is specific to each command, it is declared as abstract. It is up to the individual command, to generate its own execution context. For instance, the `AddCircleCommand` includes the following details in its generated execution context:

- The circle identifier
- The center point identifier and an identifier for the point on the perimeter of the circle
- Boolean flags (exists, showing)
- Foreground & background rendering styles
- Label details: position vector, flags (exists, showing), style and label object identifier

A partial output of `AddCircleCommand`'s opcode method is shown as a string of key-value pairs delimited by '&' below:

```
AddCircle&objectName=C8&objectExists=true&objectShowing=true&
        circleCenterPointName=P2&circlePointOnCircleName=P8
```

The `opcode()` method must also be implemented by the `CommandGroup` class, so all the individual commands in a group produce their execution context. For instance, the opcode output a group of commands that create a circle with a center is an array of strings such as shown below:

```
["AddPoint&objectName=P2&pointVector=(0.12333,0.82231,0.25833)",
  "AddPoint&objectName=P3&pointVector=(0.87225,0.01672,0.62244)",
"AddCircle&objectName=C2&circleCenterPointName=P2&circlePointOnCircleNam
                            e=P3"]
```

Figure 8. *toOpcode() Implementation in CommandGroup*

```
abstract class CommandGroup extends Command {

    toOpcode(): null | string | Array<string> {
        const group: Array<String> = []
        this.subCommand.forEach((cmd:Command) => {
            const converted = cmd.toOpcode() as null | string
            if (converted !== null) group.push(converted)
        }
        return group.length > 0 ? group : null
    }
}
```

Storing Geometric Construction Scripts

For a typical construction, the result of calling `dumpOpcode()` is a (huge) JSON array of the command script which can be saved as a string in the cloud database. When the string length is below the maximum limit allowed by Firebase Firestore, the JSON array is stored directly as string in a Firestore document. Otherwise, we apply the GZIP data compression algorithm on the JSON array and save it as binary data to Firebase Storage.

When a saved construction is loaded from the cloud database and a global parser inflates the JSON string and then determines which `Command` subclass to dispatch for parsing a specific command and thus replaying its execution context. Since the command history records the exact order how geometric objects were created, parent-child dependencies in the DAG of object tree are reconstructed correctly during the replay. The task of interpreting a construction script is implemented across several functions:

- The `run()` function initiates the entire process of command interpretation. The incoming argument to this function is an array. Each item in this array can be either a string (representing a single command) or an array of strings (representing a group of commands).
- The `interpret()` function executes each command either as a single execution or a group of executions.
- The `executeIndividual()` function's role is to dispatch the proper parser based on the command name, thus converting a string encoding of a command back to a Command object. Essentially, `executeIndividual()` performs the inverse of `toOpcode()` where it turns a Command to a JSON string.

Figure 9. *Parsing and Interpreting Geometric Construction Scripts*

```
type ConstructionScript = Array<string | Array<string>>

function run(script: ConstructionScript) {
    script.forEach ((s: string | Array<string>) => {
        interpret(s)
    })
}

function interpret (command: string | Array<string>) {
    if (typeof command === "string") {
        executeIndividual(command).execute()
    } else {
        const group = new CommandGroup()
        command.forEach((cmd: string) => {
            group.addCommand(executeIndividual(cmd))
        })
        group.execute()
    }
}

const NODULE_DICTIONARY = new Map<string,SENodule>()
function executeIndividual(command: string): Command {
  const tokens = command.split("&")
  switch (tokens[0]) {
    case "AddPoint":
      return AddPointCommand.parse(command, NODULE_DICTIONARY)
    case "AddCircle":
      return AddCircleCommand.parse(command, NODULE_DICTIONARY)
    // many more cases
  }
}
```

Most of the command subclasses either create or remove objects from the global state. When a command has one or more dependencies (to the existing objects), this command must be able to locate its dependent objects. When the `parse()` function is invoked a dictionary of objects created so far is passed (`NODULE_ DICTIONARY`) as the second argument of the call. Each `parse()` function must be implemented as a static function since we cannot invoke it from an existing object. The snippet of the `parse()` function of `AddPointCommand` is shown in Figure 10.

Conclusions

Incorporating various design patterns into Spherical Easel has enabled us to be very productive in building a significantly large number of features (32 tools) within a relatively short period of time (three fulltime summer semesters since April 2020). Summer 2023 was mainly used for migrating VueJS from version 2.0 to 3.0. Encapsulating individual spherical construction as a Command object gives

us the capability to create the foundational building blocks for several important features in Spherical Easel, this includes:

Undoing graphical edits without having to explicitly saving (and later restoring) the rendering state of the drawing canvas. Instead of saving graphical properties and values to restore, we save the "recipe" (actions) to restore them.

The "recipes" can also be transcribed into a machine-readable format (JSON string) which can saved to persistent storage.

Since saved "recipes" are machine readable, they can be interpreted, and graphical objects can be rebuilt.

Adding new objects and tools to expand the "ingredients" for each recipe is easy. The Composite design pattern enables us to group several (primitive) actions which must be performed collectively together in a single execution context.

Figure 10. *Parsing the AddPoint Command*

```
class AddPointCommand: Command {
  static parse(command: string, objMap: Map<string,SENodule>) {\
    const tokens = command.split("&")
    const propMap = new Map<string,string>()
    tokens.forEach((token,ind) => {
        if (ind == 0) return
        const parts = token.split("=").  // split the key-value
        propMap.put(parts[0], parts[1])
    })
    const sePointLocation = new Vector3()
    sePointLocation.from(propMap.get("pointVector"))
    const sePoint = new SEPoint()
    sePoint.locationVector.copy(sePointLocation)
    const pointName = propMap.get("objectName")
    objMap.put(pointName, sePoint).  // (*) Update the dictionary

    return new AddPointCommand(sePoint, /* more args */)
  }
}
```

Future Work

Spherical Easel is a work in progress, and we have a long list of features we are planning to implement including:

More tools,

A classroom mode where a teacher can view, comment, and pause all their students' work,

An electronic system for vetting and distributing lessons plans for students of all ages,

An earth mode which allows users to explore the geography of the earth,

Building on the i18N package to simplify the process of translating it into more languages, and

Implementing a more robust system of rendering and interacting with spherical parametric curves.

We have also involved students at several stages in the process of creating Spherical Easel. The lead authors are full time faculty members with a substantial teaching load and so time to work on the application during the academic year is very limited. In order to maintain continual progress throughout the academic year, we invite senior students in our Capstone course to contribute to the project. Additionally, in summer 2023, we were able to secure a research grant to fund a summer project which involves a collaborative team of faculty and students across three disciplines: mathematics, computer science, and visual & media arts to improve Spherical Easel usability and navigability as well as adding the new Earth Mode. The visual & media team started with the previous UI design (Figure 11) and made recommendations that were implemented by the computer science team that resulted in the current UI (Figure 1). In addition, the computer science team implemented an Earth Mode (Figure 12**Figure 12**) that, for instance, allows the user to:

- Create new points associated with physical geographic locations on the earth.
- Measure distances between those locations.
- Measure angles among any three locations.

Teacher Session Control

We also have experimented with implementing a feature where a teacher creates a "session" in Spherical Easel where students can join. Spherical constructions initiated by the teacher are broadcast and made visible on the students' spherical easel canvas. All these experimental features are heavily built on top of the Command pattern in conjunction with the Socket.IO library. Instead of "saving" the commands to persistent storage, the commands are transmitted to and reinterpreted by the students' spherical easel instance. The overall visual effect is the teacher's actions on his/her graphical canvas are replicated on each student canvas.

Figure 11. *The First Version of Spherical Easel UI Design*
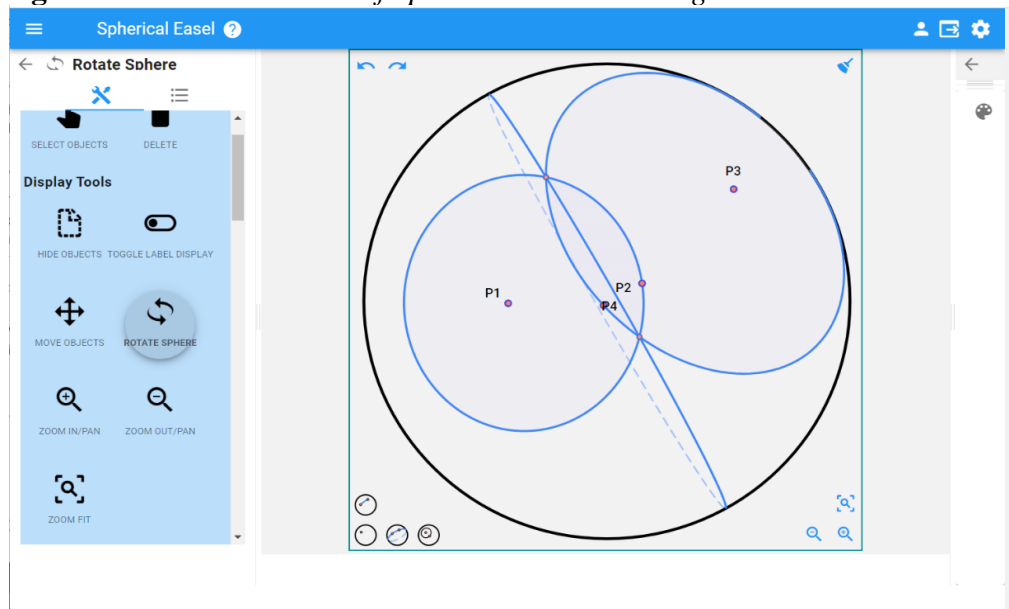
The project source code is available on GitHub (https://github.com/dulimarta/spherical-easel) and has been deployed to Netlify. The web application itself can be accessed at https://easelgeo.app. One of the main reasons we keep our code on GitHub is to invite other collaborators to our project.

Figure 12. *Earth Mode in Spherical Easel*

Acknowledgments

originator of the idea to store the relationships between geometric objects in a directed acyclic graph.

References

Back K (1997) *Smalltalk Best Practice Design Patterns*. Prentice-Hall.

Desmos Geometry. [Online.] Available at: https://www.desmos.com/geometry.

Dulimarta H, Dickinson W (2023) Spherical Easel: An Open-Source Web Application Modeling Spherical Geometry. In *III International Conference on Electrical, Computer, and Energy Technologies (ICECET 2023)*. Cape Town, South Africa.

Firebase. [Online.] Available at: https://firebase.google.com.

Gamma E, Helm R, Johnson R, Vlissides J (1995) *Design Patterns: Elements of Reusable Object-Oriented Software*. Addison Wesley.

Geogebra Geometry. [Online.] Available at: https://www.geogebra.org/geometry.

Górski T (2024) Smart Contract Design Pattern for Processing Logically Coherent Transaction Types. *Applied Science* 14(6): 2224.

Java Design Patterns. [Online.] Available at: https://java-design-patterns.com/patter ns/.

Oliveira Marum JP, Cunningham CH, Jones AJ, Liu Y (2024) Following the Writer's Path to the Dynamically Coalescing Reactive Chain Design Pattern. *Algorithm* 17(2): 56.

Node-GZIP. [Online.] Available at: https://npmjs.com/package/node-gzip.

NonEuclid - Hyperbolic Geometry. [Online.] Available at: https://www.cs.unm.edu/~joel/NonEuclid.

Nystrom R (2014) *Game Programming Patterns*. Genever Benning.

Schmidt D, Stal M, Rohnert H, Buschmann F (2000) *Pattern-Oriented Software Architecture, Volume 2: Patterns for Concurrent and Networked Objects*. John Wiley & Sons.

Todhunter I (1859) *Spherical Trigonometry, for the use of colleges and shcools.* London, England: Macmillan.

Impact of Supply Chain Disruptions and Inflation on the Construction Industry in the Arab States of the Gulf Cooperation Council

By Alan Atalah[*] & Walid Al-Azanki[*]

During the years of 2022-2023, the world economy encountered the significant challenge of supply chain disruptions due to COVID 19, Russia's invasion of Ukraine, and government subsidies during 2020 and 2021. In addition, COVID 19 disturbed the balance of the labor market; many workers retired, changed professions, moved, etc. creating a shortage of workforce. The supply chain disturbance and labor shortage lead to inflation rates that have not been seen for 40 years. The construction industry is a significant part of the any country's economy including the Gulf Cooperation Council (GCC) countries which is composed of: United Arab Emirates, Bahrain, Kingdom of Saudi Arabia, Sultanate of Oman, Qatar, and Kuwait. It is hypothesized that the GCC States are immune to such supply chain and inflation drivers due to the oversupply of imported work force and the economic prosperity that these countries enjoy. Is the construction sector, which is one of the leading economic sectors in the GCC region also immune as well? This paper attempts to examine this hypothesis through a survey designed to capture the opinions of construction professional operating in these states. This survey attempts to

- *Examine the impact of supply chain disturbance, labor shortage, and inflation on the construction industry in the GCC countries.*
- *Figure out how the construction industry reacted to and dealt with these challenges.*

The findings of this research would give us a snapshot of the state of the construction industry and help the industry deal with the above-cited challenges.

Keywords: *Inflation, supply chain, construction industry, and Gulf Cooperation Council (GCC)*

Introduction

This section provides the reader with a generic overview of the geographic, historical, and economical nature of the Gulf Cooperation Council (GCC) region. The GCC is the natural progression of the shared history, religion, and culture along with the prevailing kin relations among the citizens of its countries. GCC is a practical answer to the shared challenges of security and economic development in the region (Encyclopaedia Britannica 2023). In May 1981, the leaders of

---

[*]Professor, College of Technology, Architecture and Applied Engineering, Bowling Green State University, USA.
[*]Assistant Engineer, Turner Construction, USA.

Bahrain, Kuwait, Oman, Qatar, Kingdon of Saudi Arabia (KSA), and the United Arab Emirates (UAE) established a cooperative framework to enhance coordination, integration, and inter-connection among these states to unify, deepen and strengthen the relations and cooperation among their citizens (Gulf Cooperation Council 2023). In addition, being one geographical entity have facilitated contacts and interaction among its citizens and have created homogeneous values and characteristics (Encyclopaedia Britannica 2023).

GCC aims to formulate similar regulations in economic/financial affairs, commerce, customs, communications, education, culture, health care, information, tourism, and legislative/administrative affairs. It also seeks to stimulate scientific and technological progress in the fields of industry, water, mining, agriculture, and animal resources. The council also encourages cooperation in scientific research and joint ventures for the good of their peoples (Gulf Cooperation Council 2023).

The Arabian Peninsula is a desert environment surrounded by saltwater bodies: Persian Gulf, Arabian Sea, and Red Sea as shown in Figure 1. KSA, which is the largest member of the GCC, receives only four inches of precipitation per year on average. The southern portions of the peninsula are some of the hottest places on Earth. Summer temperatures can reach more than 120º F. There are no natural lakes or significant rivers on the peninsula. Historically, the region is extremely dry with low population density, though oil discoveries increase the population density in the region (Dastrup 2019). The GCC states are small open economies with high dependence on international trade; they export oil and natural gas and import almost all the material and supplies needed to sustain a high standard of living for 58.86 million capita (WorldData.info 2024). The high dependence on international trade makes them vulnerable to global and domestic shocks (Rezghi et al. 2023).

Figure 1. *Map of the Gulf Cooperation Council (GCC) Countries (Encyclopaedia Britannica 2023)*

The GCC states supported Egypt and Syria in the war of October 6, 1973, against Israil through forcing oil embargo on the countries that supported Israil. The oil embargo tripled the oil prices within a span of a few years as shown in Figure 2 providing these states with a significant increase of GDP. The GCC rulers invested the cash surplus in improving the standard of living for their citizens through massive infrastructure projects and subsidizing education, health care, and other services. After achieving some level of prosperity, the GCC steered their resources towards diversifying their economy to sustain continuous prosperity when the oil era ends. Consequently, trillions of dollars were invested in this region over the last half a century miraculously transforming these countries from empty deserts to developed states with some high standard of living. This accomplishment is highly commendable and admirable.

Figure 2. *Oil Prices during from 1970 to 2015 (Decressin 2012)*

The rest of this paper is structured according to the following headings:

1. Literature review of the
   a. Labor and material procurement in the GCC countries.
   b. potential reasons for global inflation and supply chain disruptions.
   c. nature of the construction sector in these countries and its magnitude.
   d. inflation and supply chain in challenges in the GCC countries.
2. Research questions
3. Research methodology
4. Survey results and finding
5. Research conclusion and recommendation
6. Acknowledgement
7. References

Literature Review

The above-mentioned investments created a huge demand for workforce of all kinds and for material, equipment, and services. The huge demand combined with the extreme heat forced the GCC firms to pay premium salaries and wages to their workers, making the GCC an extremely attractive place for people to work. The creative business leaders of GCC countries created a business model with which they imported workforce from all over the world and synchronized their efforts to change these countries from empty desert to what it is today.

Labor and Material Procurement in the GCC Countries

Due to the desert nature of the GCC region, low-density population, and oil-revenue surplus; these countries relied on imported labor workforce from all over the world. The governments and citizens of these countries created an entrepreneurial model through which they attracted and managed highly-skilled professionals from the developed countries (such as UK and USA), middle-level professionals from the Middle East (such as Egypt, Jordan, Turkey, Syria, and Lebanon) and other developing countries, and low-skill workforce from neighboring developing countries such as India, Pakistan, Afghanistan, Bangladesh, Philippines, Egypt, Sudan, Syria, Lebanon, etc. They also attracted, recruited, and managed high talents and skills from all over the world, but the above-cited model represents the main skeleton of the economic development and transformation during the last half century.

They used the kafala (sponsorship) system which gives private citizens and companies in GCC almost total control over the employment and immigration status of their migrant workers. The system arose from the above-cited growing demand for cheap labor in GCC and the desperation of many migrants (seeking work) to send money home to their families back home. Some employers abused the kafala system leading to human rights abuses, racism, and gender discrimination. The preparation for the 2022 FIFA World Cup in Qatar combined with the global anti-racism protests and the COVID-19 pandemic exposed the flaws of the kafala system and fueled calls for reforms (Robinson 2022).

Potential Reasons for the Global Inflation and Supply Chain Disruptions

During the period from 2000 to 2023, most productive countries around the world went through several events that changed the economic landscape and introduced significant economic challenges that drove the economic policy makers to take certain actions. Chief among these actions is the adjustment in the central bank interest rates. The 9/11 attack (on the World Trade Center in New York and the pentagon in Washington, DC) along with the bursting of the internet bubble of the late 1990s significantly slowed down the US economy. Consequently, the federal reserve lowered its interest rate (which governs the banking lending rates) as shown in Figure 3. While the recession of 2008 was caused by creative financial engineering orchestrated by financial investments banks, it created mortgage crises

that paralyzed many global banks. This fiscal crisis significantly slowed down the world economy and kept inflation at historic low levels. The major central banks pumped trillions of dollars into their economy and kept their basic interest rates slightly above zero to avert severe recession for most of the years from 2009 to 2020.

Figure 3. *The Monthly Federal Reserve Rates from 2000 to 2023 (Board of Governors of the Federal Reserve System (US) 2023)*
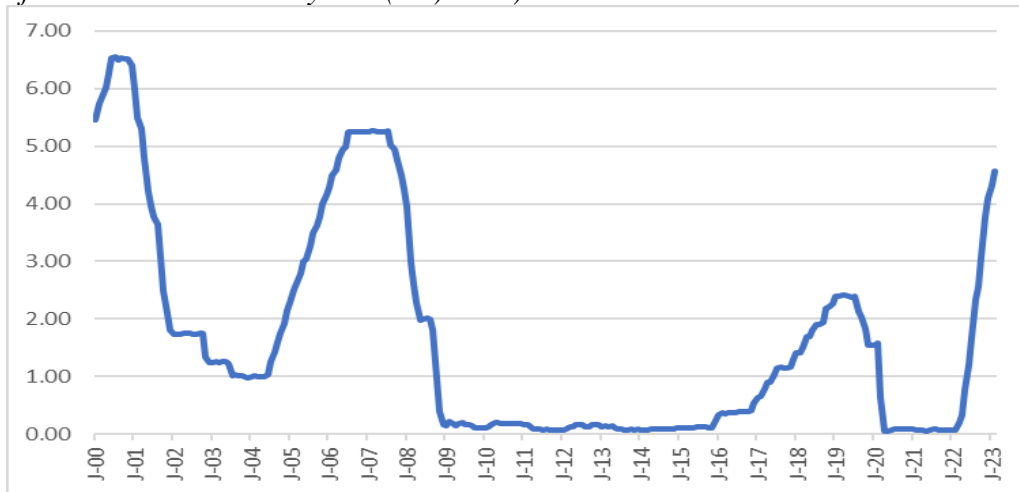
After the collapse of the Soviet Union, the world economy slowly changed from a bipolar trade to global trade. Businesses and governments built supply chains for the needed goods and services that exploited intellectual resources in the developing countries, cheap labor in developing countries, and global raw material. The admission of China into the World Trade Organization in December 2001 accelerated the perfection of the manufacturing supply chain creating an environment of low inflation. The lower cost of shipping goods from a manufacturing facility to the next facility assisted in creating very specialized manufacturing facilities all over the world with China gaining the lion share of this manufacturing. Over time, the supply chain (for goods and services in a globalized economy) has been gradually finetuned and almost reached perfection. Producers outsourced manufacturing functions and invested in facilities in areas with low-cost labor; they also outsourced some design, management, and customer services overseas further reducing production cost. The digital technological revolution that enabled cheap audio, video, and data transfer accelerated the outsourcing process. In addition, competition among producers and sellers kept prices at bay. Consequently, inflation was contained in the range of 2-3% during this period. The combination of historic low interest rates and low inflation created a goldy lock environment which created sustainable economic growth in most of the world. The perfection of the supply chain enabled China to maintain economic growth rates exceeding 7% per year and partially kept inflation at bay in the US and European Union during this period. China, consequently, lifted more than 300 million capita from poverty to middle class and created a class of millionaires and billionaires.

A supply chain disruption is any event that causes a disruption in the production, transportation, or distribution of products due to natural disasters, regional conflicts, and pandemics (Arena, a PTC Business 2023). The above-mentioned supply-chain perfection made the world economy more vulnerable to supply chain shocks. The COVID-19 epidemic forces many countries (all over the world) to shut down their economy during the first half of 2020 due to lack of knowledge about virus and high death rate. During the rest of 2020 and a good part of 2021, manufacturing all over the world kept on sputtering as many workers worked from home and only essential workers were working in the factories. China kept combating the virus by using the zero Covid policy that led to complete shutdown of large provinces, counties, and townships in 2020 and 2021. In addition, China prioritized Chinese industrial needs over international needs; this was evident in the medical supplies. The shutdown created many supply chain bottle necks that the manufacturing sector had to deal with. In the addition to the supply chain disruption by COVID-19, Russia's invasion of Ukraine and the sanctions imposed on Russia along with the blockage of the Black Sea worsened the supply chain disruption and increased inflation throughout the entire world.

In early 2022, the US and the industrialized world, started to gain confidence about dealing with COVID-19. More than half the population has been vaccinated (and postered) and a good part of the other half has developed some immunity because they have been infected with the virus. The whole US and the industrialized nations simultaneously tried to operate at full capacity as much as it can. However, the supply chain shocks due to COVID-19 and Russia's invasion of Ukraine hampered the world's ability to operate at full capacity. The authors hypothesize two more driving forces for inflation:

(1) The rich countries pumped trillions of borrowed-governmental dollars into their economy to prevent great depression. These funds created excessive capacity to purchase goods and services once the fear of COVID-19 subsided.

(2) Misjudgment of the central banks, world wise, about the sticky nature of inflation in late 2021 and early 2022 as they diagnosed this inflation as transitory. The delayed response of the central banks, due to the fear of recession, exacerbated the inflation to a level that has never been seen since the late seventies.

Despite the efforts of global governments to reduce laying off workers, businesses laid off a good percentage of their workers to offset reduced sales. Many of the laid off workers changed their career and/or relocated to lower cost areas. In addition, the workers, who were close to retirement, retired. Consequently, when the businesses attempted to reach full production capacity, they did not find the needed workforce in terms of quantity and quality. Consequently, businesses were forced to offer higher wages and salaries to attract workers, increasing the production cost.

Nature of the Construction Sectors in the GCC Countries

The governments of the GCC countries use construction projects to increase employment and foreign investments and to meet the transformational and developmental aspirations of their citizens. Consequently, the construction sector is one of the top three sources of employment in the GCC countries employing many local, foreign, and expatriate workforces. KSA is one of the leading cement producers worldwide, and much of the produced cement is mainly supplied for domestic use. Qatar is another considerable producer of cement in the region (Statista Research Department 2023).

Statista Research Department (2023) states that most of the construction investments in the GCC region were in residential and commercial buildings, followed by energy and infrastructure projects. The first phase of KSA's mega project Neom, is expected to be completed by 2025, worth 500 billion U.S. dollars. Among the recent major construction investments were the Etihad Rail projects and the Gasoline and Aromatics projects in the UAE, which made the UAE an important player in the global construction industry. The stadiums and the infrastructure projects needed for Qatar to host the soccer FIFA 2022 World Cup were among the major construction projects in the region (Statista Research Department 2023).

Figure 4. *The World's Mega Projects (Arabian Business 2023)*

Katharina Buchholz, Data Journalist with Statista, stated that many of the recent global megaprojects have centered on the Arab Gulf Region (Buchholz 2023). Figure 4 lists these top ten global megaprojects; five of these projects are in the GCC. Madinat al-Hareer (Silk City) in Kuwait: $132 Billion is one of the top 5 most expensive construction projects in the world (1build staff 2021). The value of the current projects in GCC exceeds $100 billion (Statista Research Department

2023). The Arab Monetary Fund (AMF) said that the Arab construction sector has recovered from the impacts of the Covid-19 pandemic, with its contribution to GDP in 2021 amounting to around $186.8 billion, up from $178.3 billion in 2020, or a 4.7% increase. The KSA and UAE construction sectors contributed the most to their countries' GDPs, with around $45.5 billion and $36.8 billion, respectively. In Qatar and Oman, the construction industry contributed $24.1 and $6.4 billion respectively (Mohamed 2022). The NEOM city-being built in Northwestern Saudi Arabia- is expected to be the first construction megaproject with a cost exceeding $1 trillion. NEOM in Saudi Arabia and Silk City in Kuwait are two of the biggest planned construction projects globally (Arabian Business 2023).

Paul Griffiths, CEO of Dubai Airports announced that the start of phase 2 of Dubai World Central - Al Maktoum International Airport's (DWC) expansion, representing a substantial investment of 128 billion UAE Dirham ($34.85 B). After the completion of phase 2, DWC will be a state-of-the-art airport that will provide a quick, convenient, and high quality 21st century experience for its customers. This further solidifies Dubai's strategic goal of becoming a leading aviation hub on the world stage (Griffiths 2024).

Construction Material Prices over the Last Five Years

Because the construction industry is one of the largest single industries in most countries, it is natural to theorize that the above-cited inflation and supply chain disruptions affect the construction industry. Figure 5 illustrates the consumer price index along with the construction material price index using the year 1990 as 100. The graph (whose raw data was obtained from the Federal Reserve Economic Data) illustrates that inflation of the construction material (during the period from 2021 to 2023) was higher than consumer price index, which is the highest for the last 50 years. While the data in Figure 5 is obtained from the US, these prices mirror the global prices due to the open nature of the US economy.

Figure 5. *Consumer Price Index (Federal Reserve Economic Data 2023) & Construction Price Index (Federal Reserve Economic Data 2023)*
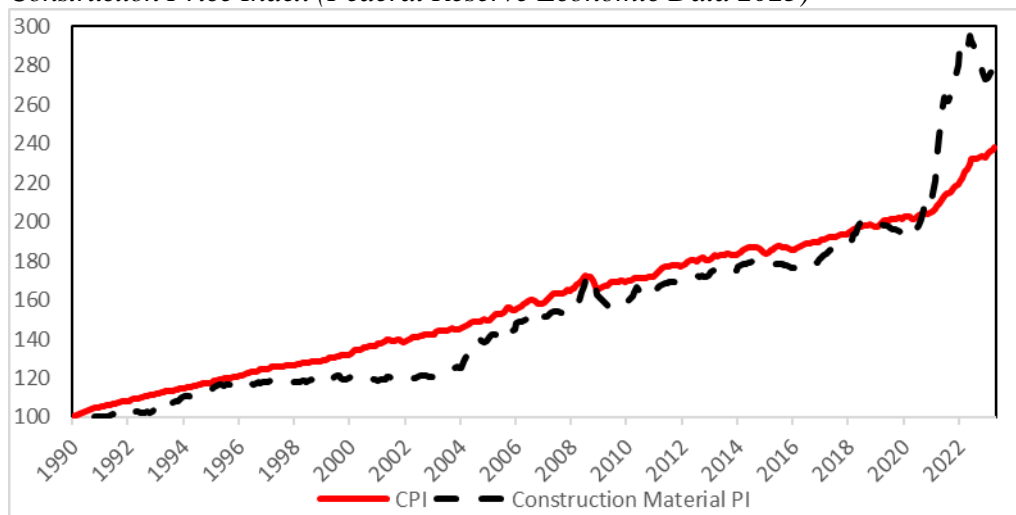
Lumber, concrete, and rebar are major construction material world wide. Figure 6 presents the softwood lumber prices and ready-mix concrete prices during the period of 2020 to 202 in the US (Logan 2023). The figure shows that the lumber prices increased significantly during the second half of 2020, then they went down twoards the end of 2020 and beginning to 2021. The prices climbed up and down again later in 2021 and they gad a similar cycle again in 2022. In part, these ups and downs in lumber and many other material gave credit to the conclusion that inflation is transatory not sticky during the second half of 2021. This ups and downs in essential construction material like lumber provided a challenge to construction project manaers. On the other hand, the ready-mix concrete prices were in steady increase during the same period.

Figure 6. *Softwood Lumber Prices (left) and Ready-mix Concrete Prices (right) 2020-2023 in the US (Logan 2023)*
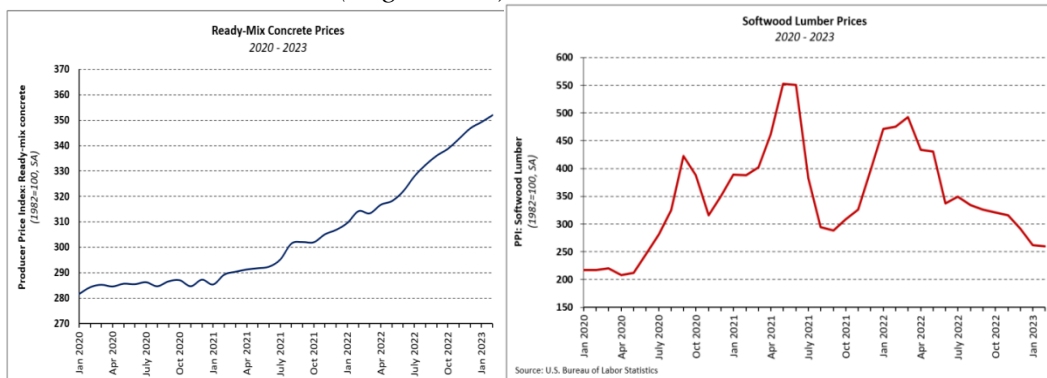
Gilbane Building Company (in its Construction Market Conditions Report-Q2 2022) reported the amount of delay of several construction materials as shown in Figure 7. The electrical and HVAC material and equipment experienced the highest level of delays because much of these materials and equipment are unique to the specific projects and are manufactured to order due to their cost and manufacturing complexity (Gilbane Building Company 2022).

Figure 7. *Building Material and the Amount of Delay (Gilbane Building Company 2022)*

Material	Lead Time
Generators	72-95 weeks
Switchboards	45-80+ weeks
Chillers	42-52+ weeks
AHUs	40-75 weeks
Panelboards	30-52+ weeks
Switchgear	30-80+ weeks
International Fabricated Millwork	24-28 weeks
Elevators	20-48 weeks
RTUs	20-30 weeks
Curtainwall	14-28 weeks
Steel	12-30 weeks
Roofing (Select Materials)	4-20 weeks

The supply chain disturbance unbalanced the supply and demand forces leading to an increase in the prices of building material and equipment. Figures 8 and 9 present the changes in material prices of the essential construction material during the period from Q4 2020 to Q4 2022 based on the Cost Index - Chicago Q4 2022 (McGreal & Van Anne 2023).

Figure 8. *Material Pricing Change Q4-20 to Q4 22 (McGreal & Van Anne 2023)*
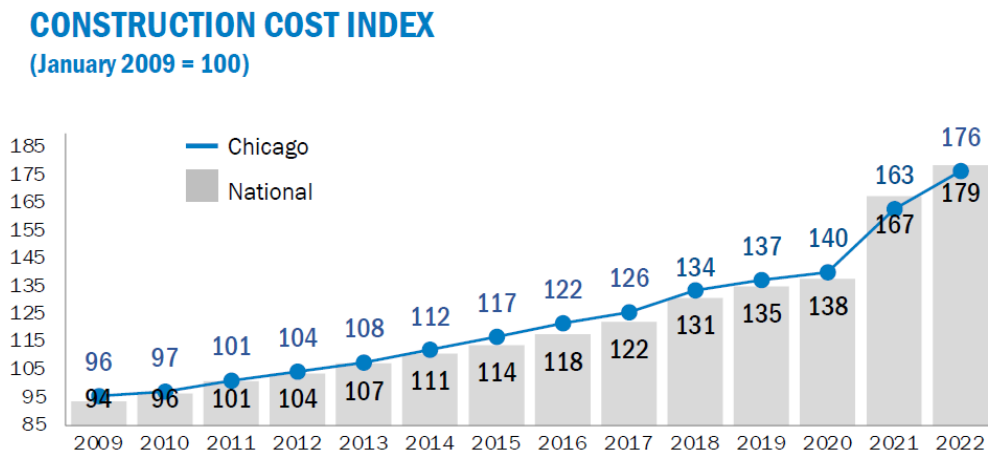
Figure 9. *Material Pricing Change Q4-20 to Q4 22 (McGreal & Van Anne 2023)*
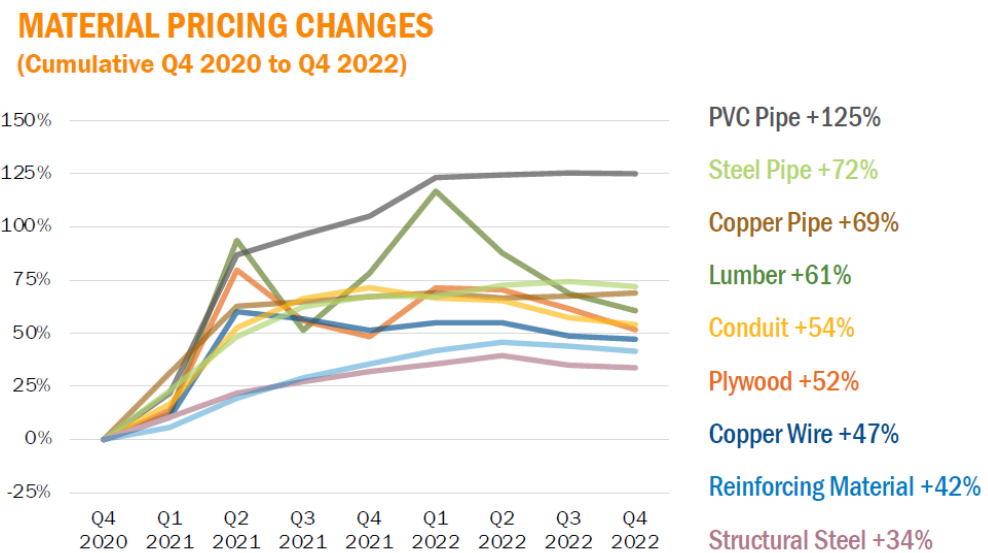
Inflation and Supply Chain Challenges in the GCC Countries

Because of the desert and climatic nature of the GCC countries, these countries heavily rely on imported goods and international trade. Theoretically, this heavy reliance makes these countries more susceptible to inflation and supply chain disruptions. Inflationary pressures have intensified in the GCC countries in 2021-2022, mainly driven by the global tradeable goods inflation described earlier in

this paper. Despite this increase, inflation remained relatively contained as compared to rest of the world (Fareed et al. 2023).

Fareed et al. (2023) found that the imported inflation from main trading partners, mainly driven by China, is the main drivers of inflation in the GCC region. They also concluded that the direct pass-through of international commodity price shocks was somewhat limited, after controlling for trading partners' inflation due to the prevalence of subsidies and administered prices in the region and the adoption of the nominal effective exchange rate (NEER) monetary policy by the GCC states (Fareed et al. 2023). NEER is an unadjusted weighted average rate at which one country's currency exchanges for a basket of multiple foreign currencies. NEER is an indicator of a country's international competitiveness in terms of the foreign exchange (BYJU'S 2024). The GCC monetary policy frameworks targeting a stable exchange rate seem to have contributed to stabilizing inflation (Rezghi et al. 2023).

Inflation in the GCC countries has remained relatively stable (below 3% on average) over the past decade. However, inflation picked up some steam in several GCC countries since the end 2021, mainly due to an increase in food and transport prices as shown in Figure 10 (Rezghi et al. 2023).

Figure 10. *Consumer Price Index in the GCC Countries, USA, and the World from 2012 to 2022 (Rezghi et al. 2023)*

Furthermore, food and transport are major drivers for inflation increases in 2021 and 2022. Food inflation has increased from 2.2 percent (y/y) in April 2021 to 6 percent (y/y) in June 2022. While inflati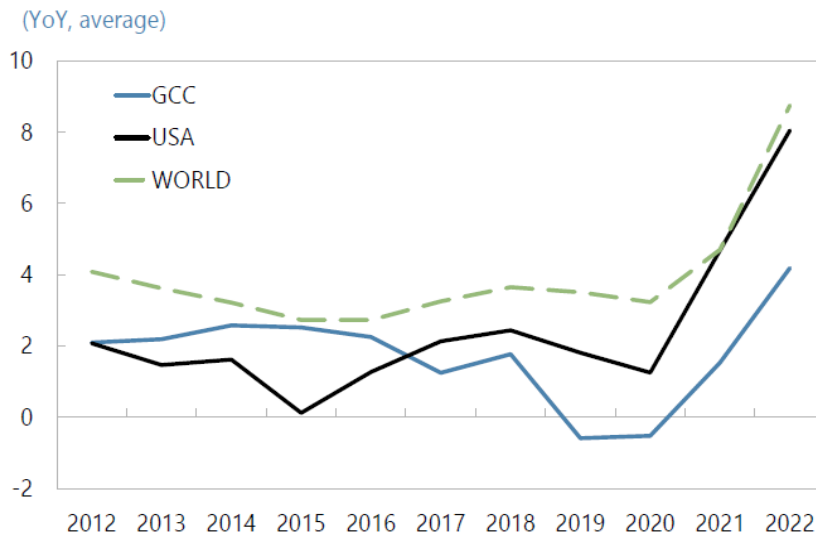on has been on an upward trend, it remained below neighboring countries in the Middle East and North Africa. The prevalence of administered prices and subsidies may explain these inflation differences. Figure 11 depicts the inflation by category in the GCC countries from August 2019 to April 2022.

Figure 11. *Inflation by Category in the GCC Countries from August 2019 to April 2022 (Rezghi et al. 2023)*
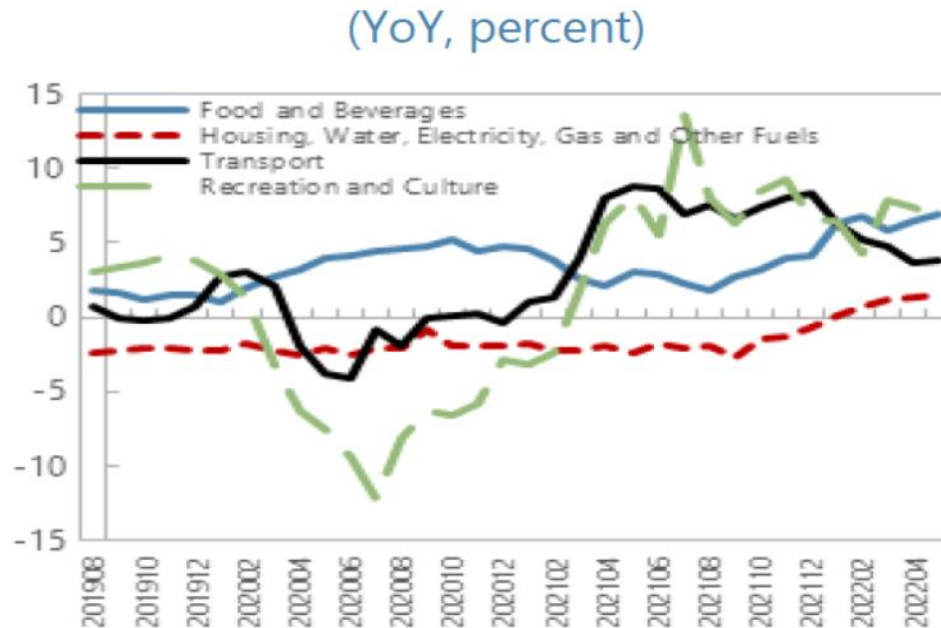
Considering the magnitude of the economy of these countries and size of the construction sector in these countries, capturing a snapshot of the industry after COVID-19 and its disturbance to the supply chain and inflation along with investigating how the industry reacted to this challenging environment is beneficial to the construction industry. The rest of the paper presents the research design criteria, implementation, findings, and results.

Research Questions and Methodology

The anecdotal conversations with many construction professionals about supply chain disturbance (combined with high inflation) motivated the authors to research their impact on the construction industry in the GCC and how the industry reacted to these forces. The literature review confirmed these forces along with their macroeconomic magnitude, but the impact of these forces on the different parties of construction projects was not documented. How the different sectors of construction industry experienced these disturbances. How much the material/systems components of the construction projects have been impacted? Did the size of the construction firms make a difference in the magnitude of impact? It is also interesting to learn how construction firms reacted to these forces and operated in this environment.

Research Methodology

In addition to reviewing literature about inflation and supply chain disruptions, asking the construction professional who dealt with these disturbances to inform

us about their impact gives us another insight. The authors developed a survey to collect the answers to these research questions. The survey, which is included in Exhibit 1, is composed of the following sections:

- Demographic questions to see if the impact differs among the subjects based on the different types of construction work, the subject's role in the project, and the sales volume of the subject's firm.
- The magnitude of the impact of the different construction material and equipment.
- The extent of wage increases to the firms' labor workforce along with the type of workforce that got bigger increases.
- The amount of the impact on the construction schedule, budget, profitability, and quality.
- The severity of the impact of labor shortage, losing loyal skilled workers, and project termination
- The implementation of the escalation clauses to adjust the contract's prices and durations.
- The adjustments by the estimating department to raise the cost of material and labor in their estimating data basis.
- The adjustments made by the prices by competing firms.

It was important to ensure that the duration of answering the survey was less than 10 minutes to facilitate responding to the voluntary survey. The authors eliminated time consuming questions and fill-in questions and combined questions to reduce the survey duration. Then the authors piloted the survey to assess its duration and to ensure that the subject interpreted the questions according to the intended meaning. Based on the provided feedback, the authors modified the survey instrument; the final survey instrument is Appendix I. Because this research involves human subjects, the Institutional Review Board (IRB) at Bowling Green State University reviewed and approved the survey prior to its distribution. The researcher used Qualtrics XM platform to create, distribute, and analyze the survey.

At least 400 construction professionals living and operating in the GCC countries were invited to respond to the survey in both English and Arabic. These construction professionals were personal contacts to the authors and their personal contacts. The authors sought the assistance of several associations such as Me3margi, Lean Construction Institute – Qatar (LCI Qatar); LinkedIn posts got over 3200 impressions that helped spread the word. We ended up with 54 valid responses despite all the efforts to increase the response rate constituting a response rate of 13.5%.

Survey Results and Finding

Demographics of the Survey Subjects

68% of the respondents worked for Engineering/Architectural firms, 29% worked for General Contracting firms, and 3% of the respondents worked for subcontracting firms. This may have skewed the subjects towards the Engineering/ Architectural firms, which may not have intimate relationships with material supply shortage. The firms (for which the subjects were working) were involved in variety of types of construction; their distributions (which is shown in Figure 12) were as follow: 44% of the respondents engaged in residential construction, 44% were involved in commercial construction, 53% engaged in heavy construction (such as infrastructure and roads and bridges), and 41% were involved in residential/ commercial towers. Please note that the summation of all the percentage is more than 100% because some firms participated in more than one type of construction.

Figure 12. *The Respondents' Type of Construction*
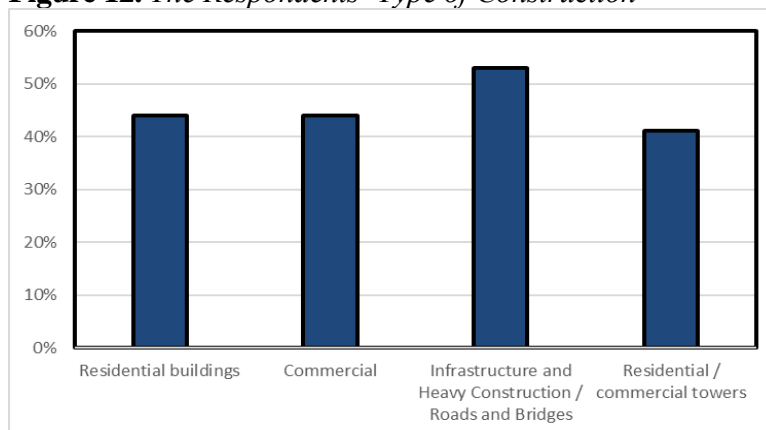
The sales volume distribution of the respondents is shown in Figure 13. 72% of respondents have a sales volume that exceeds 30M Riyal, which is equivalent to around $8M. This may have skewed the subjects towards the larger side of firms. The currencies of the GCC states are relatively close to each other except the Kuwaiti Dinar, which is around 12-13 time the Riyal. Consequently, we created a separate version of the survey for the Kuwaiti construction professionals. The numbers and percentages shown in the Figure are adjusted to the Kuwaiti equivalent in Saudi Riyal.

Figure 13. *The Sales Volume Distribution of the Respondents in Saudi Riyal*
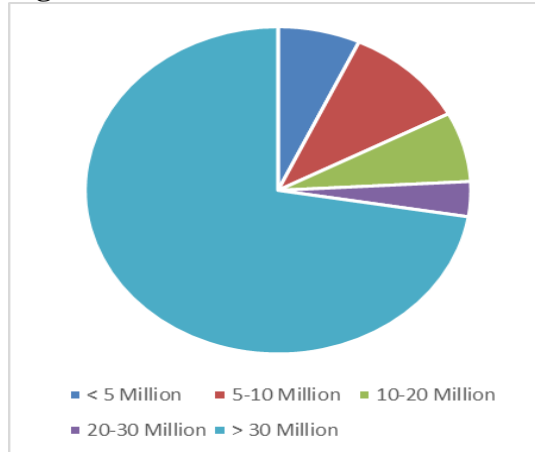
The Impact of Materials /Systems Shortage on the Business Operations

The survey subjects rated the impact of the shortage of the materials /systems (listed in Table 1) on their business on a scale of 1 (almost no impact) -5 (very severe impact) (in case the material not applicable to company work keep blank). The authors used the Likert scale, or rating system, which is a measurement method used in research to evaluate attitudes, opinions, and perceptions (Qualtrics XM 2024). In this analysis, the authors used a weight of one for minimum impact and five for maximum impact.

Table 1 presents the impact of materials /systems shortage on the business operations of the subjects on a scale of 1 to 5. Most of the impacts were between 2.6 to 3.5, which means that the subjects did not significant encounter shortage in these items because the encounter was short in duration/magnitude, and/or the encounter was easily managed. A few material items had slightly higher impact; their impact was less than 4.0. These items were electrical fixtures and equipment, plumbing fixtures and equipment, cement, and rebar. Because of the prevalent use of cement and rebar in the construction sector in these countries, any small disturbance has felt impact.

Table 1. *Weight Value for the Impact of Shortage of Construction Material/Systems on their Operations*

Material	Weighted Value	Material	Weighted Value
Timber formwork	3.23	Backfill material	3.3
Electrical wires	3.48	Asphalt	3.47
Electrical fixtures and equipment	3.6	Gabbro	3.13
Pipes	4	Polymer	2.69
Plumbing fixtures and equipment	3.93	Bitumen	3.4
Firefighting fixtures & equipment	3.32	Curb stone	3.31
HVAC system	3.2	Rebar	3.67
Glass	2.83	Interlock tiles	2.93
Moister protection material	3.21	Others:	2.54
Kitchen finishing items (ex. Cabinets and countertop)	2.59	Energy (electrical, gasoline, diesel)	3.57
Cement	3.81	Masonry	3.33

Woodwork	2.66	Flooring finishing materials	3.39
Aluminum works	2.9	Paint	3.07
Wrought iron works	2.93	False ceiling materials	2.74
Washed sand	3.07	Insulation material	3.13

The Impact Labor Shortage on the Business Operations

In their answer to question # 5, how much did your firm increase the wages of its workers during the last 18 months; 64% indicated that raised the wages of their workers by less than 5%. 18% of the subjects increased their wages between 5 to 10%, and 9% increased their wages by 10 to 20%, and 9% increased the wages of their workers by more than 20%. A potential explanation for such a slight increase in labor wages is that most of these workers were imported workers from countries whose economies were hit hard by COVID-19 and global inflationary forces explained earlier in the paper. In other words, the premium difference between their income in their own countries and their income working in the GCC countries increased significantly (even if these workers got a very slight increase).

In their response to Question 6 - Did your firm faced any shortage in manpower? 14% indicated that they did not face shortage, and 86% indicated that they faced labor shortage with most of the shortage was for skilled workers. The answers to the follow up Question # 7 indicated that 27% of the shortage was for average-skilled workers and 55% of the shortage was for the highly skilled workers.

The Impact of Supply Chain Disruptions on Their Construction Projects

In their response to Question 8-Using the table below, please indicate, where applicable, the percentage impact of supply chain disruptions on your construction projects, where 0 – 20% indicates the least impact with 81-100% the highest impact; the analysis results (using the Likert scale) are shown in Table 2. The figures in the table indicate that the impacts of supply chain disturbances were mostly slightly above average.

Table 2. *Impact of Supply Chain Disruptions on Their Construction Project*

Area of Impact	Average Score
Schedule and ability to finish the project on time	3.09
Price Inflation	3.18
Profitability/ business growth	2.81
Labor shortage	3.13
Losing loyal skilled workers	3.06
Procurement substitution	2.9
Project termination	2.52

Employment of Escalation Clauses to Adjust the Contract Price and Duration

In their response to Question 9-If your firm suffered from inflated prices and supply chain problems, did the project owner consider it as part of the contracting business risks that the contractor must absorb? 57% of the respondents indicated that the owner did not modify the contract time and/or price because of this disturbance. On the other hand, 43% indicated that the owners of their projects adjusted the contract process and saw the disturbance as a legitimate reason for a change order to modify the contract time and price.

Adjustment of the prices in the estimating databases

The responses to Question 10 - Did the estimating department in your firm update its cost to reflect the increased prices and material shortage? 75% stated that their estimating department updated its cost databases to reflect the increased prices and material shortage, 25% did not.

Question 11 - Did the competing firms to your firm update their prices to reflect the increased prices and material shortage? 72% of the respondents indicated that their competition increased their prices as well, and 28% did not see the competition raising their prices.

Future Forecast

Question 12 asked the respondents when they foresaw that supply chain disruptions would subside? 22% foresaw that it will end towards the end of 2024, 19% foresaw the subsidence by the end of 2026, 59% foresaw that it will never end; this is the new normal.

Question 13 asked the respondents how they foresaw the effects of the supply chain disruptions on the growth projections of their firms over the next three years. 42% expected a decline in the company's growth over the next 3 years, 19% expected that their company would maintain the same growth rate, and 39% expected that their firms would expand in the next three years due to the increased demand for their services.

Research Conclusion and Recommendation

The political and economic events during the last thirty years drove the global central banks to keep interest rates low for a long time to avoid economic recession. During the second half of 2022, inflation started to rise due to economic recovery from COVID-19, but global central banks underestimated the sticky nature of inflation. Ukraine war at the beginning of 2023 added fuel to the inflationary forces. Both COVID-19 and Ukraine war presented a significant challenge to the global supply chain including the construction material, equipment, and systems.

The GCC nations were able to absorb the inflationary pressure better than many other regions in the world. The GCC monetary policy framework targeting a stable exchange rate (such as NEER) and subsidies seems to have stabilized inflation. The construction sector, which is a sizable portion of the GDP of these countries, dealt with/managed the global supply chain distributions and inflation as hypothesized. The impacts of materials /systems shortages on the business operations of the subjects were between 2.6 to 3.5; which means that the subjects encounter mostly minor shortage in these items, or the shortage lasted for a short manageable period. Critical items such as cement and rebar scored an impact higher than 3.5, but less than 4.

The wages of workers in the GCC countries did not increase significantly because many of the workers in GCC were imported workers from countries whose economy were hit hard by COVID-19 and global inflationary forces. The authors hypothesize that the wages/salaries premium for working the GCC states (compared to those of working in the home countries) increased because the impact of inflation was harder in their home countries. The construction firms in GCC suffered a slight shortage of labor (mostly on the skilled labor level).

The supply chain disturbance and inflation had minimum impact on the construction operations such as schedule, business profitability, and growth. 43% of the subjects indicated that the owners of their projects adjusted the contract process and saw the disturbance as a legitimate reason for a change order to modify the contract time and price. 75% of the subjects stated that their estimating department updated their cost databases to reflect the increased prices and material shortage. Their competitors also raised their prices as well. 59% of the respondents foresaw that current prices and inflation will never end; this is the new normal. 57% of the respondents expected that their firms would expand in the next three years (or stay as they are) due to the increased demand for our services.

In the authors' opinions, the short comings of this study include the low response rate and skewed subject pool of larger firms who were mostly work for Engineering and architectural firms. Ideally, the subject pools would have more general contractors and subcontractors. Also, larger firms might have better capacity to manage supply chain disruptions than small firms did.

Research Recommendations

The authors recommend pursuing studying the effect of supply chain disruptions and inflation with respondents who mostly work for contracting and subcontracting firms. These subjects procure/manage construction material, equipment, and systems more directly than those who work for Engineering/ Architectural firms. It is also recommended to study the effect of supply chain disruptions and inflation on the construction industry in less economically fortunate countries because they may not have the capacity to deal with these issues. It is also recommended to study these effects on the construction industry in various locations across the world such as the USA and European Union.

References

1build staff (2021, April 16) *The Top 5 Most Expensive Construction Projects in the World*. Available at: https://www.1build.com/blog/con struction-projects.

Arabian Business (2023, April 9) *Saudi Arabia, Kuwait lead Gulf states in megaprojects: Report*. Arabian Business. Available at: https://www.arabianbusiness.com/industries/ construction/saudi-arabia-kuwait-lead-gulf-states-in-megaprojects-report.

Arena, a PTC Business (2023, May 23) *What is Supply Chain Disruption?* Available at: https://www.arenasolutions.com/resources/glossary/supply-chain-disruption/#:~:text =A%20supply%20chain%20disruption%20is,%2C%20regional%20conflicts%2C% 20and%20pandemics.

Board of Governors of the Federal Reserve System (US) (2023, March 16) *Federal Funds Effective Rate [FEDFUNDS]*. FRED, Federal Reserve Bank of St. Louis. Available at: https://fred.stlouisfed.org/series/FEDFUNDS.

Buchholz K (2023, April 4) *The World's Megaprojects*. Available at: https://www.statista. com/chart/29653/megaprojects/#:~:text=Out%20of %20all%20nine%20ongoing,and %20500%20meters%20in%20height.

BYJU'S (2024) *NEER and REER - Difference between Reer & Neer (UPSC Notes)*. Available at: https://byjus.com/: https://byjus.com/free-ias-prep/neer-and-reer/.

Clough RH, Sears GA, Sears KS, Segner RO, Rounds JL (2015) *Construction Contracting A Practical Guide to Company Management; Eighth Edition.* Hoboken, New Jersey: John Wiley & Sons, Inc.

Dastrup RA (2019) *Introduction to World Regional Geography.* Creative Commons Attribution-NonCommercial-ShareAlike 4.0 International License.

Decressin J (2012, May 25) *IMF Survey: Global Economy Learns to Absorb Oil Price Hikes*. International Monetary Fund. Available at: https://www.imf.org/en/News/Arti cles/2015/09/28/04/53/sonum052512a.

Encyclopaedia Britannica (2023, May 4) *Gulf Cooperation Council. International Organization*. Available at: Encyclopedia Britannica.: https://www.britannica.com/ topic/Gulf-Cooperation-Council.

Fareed F, Rezghi A, Sandoz C (2023) *Inflation Dynamics in the Gulf Cooperation Council (GCC): What is the Role of External Factors?* International Monetary Fund.

Federal Reserve Economic Data (2023, May 22) *Consumer Price Index for All Urban Consumers: All Items in U.S. City Average.* Available at: https://fred.stlouisfed.org/series/CPIAUCNS.

Federal Reserve Economic Data (2023, May 22) *Producer Price Index by Commodity: Special Indexes: Construction Materials.* Available at: https://fred.stlouisfed.org/series/ WPUSI012011.

Gilbane Building Company (2022) *Construction Market Conditions Report Q 2 2022.*

Griffiths P (2024, April 28) *Dubai Media Office.* Available at: https://twitter.com/DXBMediaOffice/status/1784536579198853304.

Gulf Cooperation Council (2023) *About GCC.* Available at: https://www.gcc-sg.org/en-us/AboutGCC/Pages/StartingPointsAndGoals.aspx.

McGreal D, Van Anne S (2023) *Mortenson Cost Index Chicago Q4 2022.*

Mohamed H (2022) *Construction industry contributed $186.8bln to Arab GDPs in 2021.* Available at: https://www.zawya.com/en/projects/construction/construction-industry-contributed-1868bln-to-arab-gdps-in-2021-odt446xb.

Qualtrics XM (2024, April 16) *What is a likert scale?* Available at: https://www.qualtrics.com/experience-management/research/likert-scale/#:~:text=A%20likert%20sca.le%2C%20or%20rating,engagement%20surveys%2C%20to%20market%20research

Rezghi A, Sandoz C, Fareed F (2023) *Inflation Dynamics in GCC.* Available at: https://thedocs.worldbank.org/en/doc/0b31178a21d35b986ecfe7d2795a88bb-0280032023/original/Inflation-Dynamics-in-GCC.pdf.

Statista Research Department (2023) *Difference between the inflation rate and growth of wages in the United States from January 2020 to April 2023.* Available at: https://www.statista.com/statistics/1351276/wage-growth-vs-inflation-us/.

The World Bank Group (2023) *GDP growth (annual %) - United States.* Available at: https://data.worldbank.org/indicator/NY.GDP.MKTP.KD.ZG?end=2021&locations=US&start=1999

Trading Economics (2023) *Lumber.* Available at: Trading Economics-Lumber: https://tradingeconomics.com/commodity/lumber.

U.S. Bureau of Labor Statistics (2023) *Employment Cost Index – March 2023.* March: US Department of Labor.

WHIO Staff (2022, September 7) *Giant Intel semiconductor plant in Ohio to create economic ripple that will reach the Miami Valley.* Available at: https://www.whio.com/news/local/giant-intel-semiconductor-plant-ohio-create-economic-ripple-that-will-reach-miami-valley/TU64PWVT3FENZJOEIMKGTZJTWA/.

World Bank (2023) *U.S. GDP Growth Rate 1961-2023.* Available at: https://www. macrotrends.net/countries/USA/united-states/gdp-growth-rate.

World Bank (2023) *US GDP Growth Rate 1960-2023.* Available at: Source.

WorldData.info (2024) *Member states of the GCC: Gulf Cooperation Council.* Available at: https://www.worlddata.info/alliances/gcc-gulf-cooperation-council.php#:~:text=The%20GCC%20is%20an%20alliance,percent%20of%20the%20world%20population.

Appendix 1. *Impact of Supply chain disruptions and Inflation on the Construction Industry in gulf region EN/AR*

This is an informed consent for the "Effect of supply chain disruptions and inflation on the construction industry in Qatar, UAE and KSA."

My name is Alan Atalah, and I am a professor at Bowling Green State University in the Construction Management Department. We are trying to study the impact of supply chain disruptions and inflation on the construction industry. We are approaching you because you are a construction professional whose experience and views are relevant to this study.

This research can help the construction industry by (1) evaluating the impact of supply chain disruptions and inflation (that the entire world experienced in 2022 and 2023) on the construction industry and (2) learning how the industry adjusted to the material shortage and inflation challenges. This is a voluntary survey without direct benefits.

We understand how busy construction professionals like you are; we deeply appreciate giving us an estimated to be less than 10 minutes of your time. After the completion of the survey, the collected data will be stored on a BGSU server. The collected data will be analyzed under my supervision to draw the appropriate databased conclusion. The risks involved in participation are no greater than those experienced in daily life.

Your participation is completely voluntary. You are free to withdraw at any time. You may decide to skip questions (or not do a particular task) or discontinue participation at any time without explanation or penalty. Your decision whether to participate will not affect your relationship with Bowling Green State University or with me. Please be advised that taking the survey indicates consent.

The survey data will be kept confidential and stored on a secured university server accessible only by me (and my graduate assistant Walid Al Azanki) with the appropriate password. The data will be kept for a year after the publication of the paper/report. This survey does not collect sensitive data; however, if you are concerned, please be aware that (1) some employers may use tracking software so you may want to complete the survey on a personal computer, (2) do not leave the survey open if using a public computer or a computer that others may have access to, and (3) clear your browser cache and page history after completing the survey.

If you have any questions, please do not hesitate to contact Professor Alan Atalah at aatalah@bgsu.edu or phone number: +(1) 419372 8354. If you have any questions about your rights as a participant in this research, please contact the Chair of the Institutional Review Board at Bowling Green State University, at +(1) 419-372-7716 or irb@bgsu.edu. Thank you for your time.

Impact of Supply chain disruptions and Inflation on the Construction Industry in gulf region EN/AR

1. What is the role of your firm in the construction industry?
    o   Engineer
    o   General Contractor
    o   Subcontractor
2. What is the major type of construction work that your firm is involved in
☐   Residential   ☐   Commercial   ☐   Infrastructure and Heavy Construction
3. What is the annual sales volume for your firm?
☐   < 5 M Riyal   ☐ $5-$10 M Riyal ☐ $10-20 M Riyal   ☐ $20-30 M Riyal
☐ >$30 M Riyal
4. Please rate the impact of the shortage of these materials /systems on your business on a scale of 1 (almost no impact) -5 (very severe impact)

Material	1 (min. impact)	2	3	4	5 (very severe impact)
Lumber					
Concrete					
Rebar					
Energy (electrical, gasoline, diesel)					
Masonry					
Flooring					
Ceiling					
Roofing material					
Insulation material					
Electrical wires					
Electrical fixtures					
Electrical equipment					
Pipes					
Plumbing and firefighting fixtures					
Plumbing and firefighting equipment					
HVAC Conduits					
HVAC finish fixtures					
HVAC equipment					
Doors and windows					
Moister protection material					
Kitchen finishing items (ex. Cabinets and counters)					

Other (please state in the line below)

5. By roughly how much did your firm increase the wages of its workers during the last 18 months?
   - ○ < 5%
   - ○ 5-10%
   - ○ 10-20%
   - ○ >20%
6. Did your firm faced any shortage in manpower? multiple answers selection is allowed.
   - ○ NO,
   - ○ Yes, in skilled labor.
   - ○ Yes, in unskilled labor.
7. What category of workers got higher wage raises?
   ☐ Low skilled workers   ☐   Middle level skilled workers   ☐ Highly skilled workers
8. Using the table below, please indicate, where applicable, the percentage impact of supply chain disruptions on your construction projects, where 0 – 20% indicates the least impact with 81-100% the highest impact.

RANGE OF IMPACT (%)	0-20 %	21-40 %	41-60 %	61-80 %	81-100 %
Schedule and ability to finish the project on time	☐ ☐	☐	☐		☐
Price Inflation	☐ ☐	☐	☐		☐
Profitability/ business growth	☐ ☐	☐	☐		☐
Labor shortage	☐ ☐	☐	☐		☐
Losing loyal skilled workers	☐ ☐	☐	☐		☐
Procurement substitution	☐ ☐	☐	☐		☐
Project termination	☐ ☐	☐	☐		☐

9. If your firm suffered from inflated prices and supply chain problems, did the project owner consider it as
   ☐ Part of the contracting business risks that the contractor must absorb.
   ☐ Legitimate reason for a change order to modify the contract time and price.
10. Did your estimating department update its cost to reflect the increased prices and material shortage?
    ☐ Yes   ☐   No
11. Did the competing firms to your firm update their prices to reflect the increased prices and material shortage?
    ☐ Yes   ☐   No

12. Do you foresee that supply chain disruptions will subside by?
    ☐ The end of 2023   ☐   The end of 2024   ☐   The end of 2025
    ☐ It will never end; this is the new normal.
13. Did the supply chain disruptions affect your firm's growth projections for the next three years?
    ☐ Yes, our growth declined slightly   ☐   No, our growth stayed the same.
    ☐ No, our growth projection increased because this is high demand for our services.

Machine Learning-Based Evaluation of Susceptibility to Geological Hazards in Yunyang District, Shiyan City, China

By Xin Zhou[*], Hao Wang[♦],
Aoxuan Tan[±], Enjing Zhang[°] & Jinxin Chong[•]

Regional geohazard susceptibility evaluation and early warning are effective means of disaster prevention and mitigation. The traditional regional geohazard evaluation has problems such as limited model accuracy and insufficient refinement. With the rapid development of big data and artificial intelligence technology, machine learning algorithms are gradually widely used in geologic hazard evaluation and have achieved better results. The paper uses BP neural network model and support vector machine model in machine learning algorithms to predict regional geologic disaster susceptibility. The paper selects Utopia District of Shiyan City, Hubei Province as the study area, constructs the evaluation database, selects the sample set, and trains the evaluation model with tuning parameter optimization. The results show that the support vector machine model has the highest AUC value and the distribution of geologic hazards in the evaluation results is more accurate. The susceptibility of geologic hazards in Utopia is divided into four categories: low susceptibility, medium susceptibility, medium-high susceptibility and high susceptibility, in which the low susceptibility area accounts for 17.11% of the total area, the medium susceptibility area accounts for 33.57% of the total area, the medium-high susceptibility area accounts for 42.94% of the total area and the high susceptibility area accounts for 36.55% of the total area. The results of the thesis research are of guiding significance for the disaster prevention and mitigation work in Shiyan City Utopia.

Keywords: *geohazard, susceptibility assessment, support vector machine, BP neural network, informativeness modeling*

Introduction

Geohazard risk evaluation can be defined as a systematic process of studying the extent to which a particular impact factor poses a hazard to human society in a given area and time. The main purpose of geohazard risk evaluation is to determine the scope of the risk and to rank the risk in order to provide a scientific and systematic method to reduce the risk. In the evaluation research, researchers

---

[*]Engineer, Tongxing (Hubei) Investment Consulting Co, China.

[♦]Senior Engineer, Geological Survey Center in Wuhan, China Geological Survey, China.

[±]Graduate Student, Faculty of Engineering, China University of Geosciences, China

[°]Graduate Student, Faculty of Engineering, China University of Geosciences, China.

[•]Engineer, China Railway Real Estate Group Zhongnan Co, China.

have directed their research goals to the improvement of evaluation accuracy in the evaluation process, and with the continuous improvement of machine algorithms, the research on the use of machine learning algorithms in geohazard analysis has been a hot topic nowadays.

Bi et al. (2014 used an artificial neural network evaluation method to establish an evaluation index system based on the analysis of the distribution and causes of landslides to evaluate landslide susceptibility in the western basin of Hunan. Tsangaratos and Bernardos (2014) used an artificial neural network in order to better simulate the nonlinear relationship between landslides and geomorphological parameters to evaluate the susceptibility of geologic hazards in the study area in two phases using an artificial neural network model to evaluate the geohazard susceptibility of the study area in two phases. In 2015, Polykretis et al. studied the various factors leading to the genesis of landslides based on 3S technology, established an evaluation index system, and evaluated landslide susceptibility using an artificial network (Polykretis et al. 2015) and in 2019, Valencia Ortiz and Martinez-Grana used a neural network model to evaluate the conditions of the degree of landslide susceptibility in Capitanijo, Colombia, and the results of the evaluation were predictive for the landslide (Valencia Ortiz and Martinez-Grana 2019). Suryana Soma et al. (2019) utilized a combination of logistic regression and artificial neural network evaluation methods to evaluate landslide susceptibility, and the prediction accuracy reached more than 90%. In 2019, Moayedi et al. applied the artificial neural network optimized by particle swarm optimization algorithm to the problem of landslide susceptibility map prediction, and the study showed that the artificial neural network optimized by particle swarm optimization algorithm had a good prediction performance (Moayedi et al. 2019).

In 2020, Bragagnolo et al. selected seven factors such as geomorphology, stratigraphic lithology, etc., and used an artificial neural network model to evaluate the susceptibility of landslide susceptibility map of Brazilian Porto Alegre and Rio de Janeiro regions for landslide susceptibility evaluation (Bragagnolo et al. 2020). The same year, Van Dao et al. investigated the development and validation of a deep learning neural network model for predicting landslide susceptibility, and the insights provided by this study will be valuable for the further development of landslide prediction models and the spatial evaluation of landslide susceptible areas worldwide (Van Dao et al. 2020). Liu et al. (2022) selected Zhangzha Town, Sichuan Province and Lantau Island, Hong Kong as the study areas to introduce a convolutional neural network (CNN)-based model for landslide susceptibility assessment, and systematically compared its overall performance with that of traditional random forest, logistic regression, and support vector models, using the ROC curve accuracy test and several statistical metrics to evaluate the model's performance. The results show that both CNN and traditional machine learning based models have satisfactory performance, and the CNN based model has excellent predictive ability and achieves the highest performance.

In this paper, two machine algorithms, BP neural network and support vector machine, are used to carry out the evaluation research of geohazard susceptibility in Utopia District of Shiyan City, combining with the evaluation results of the information quantity model, to discuss in depth the performance and differences of

the two machine learning algorithms in the evaluation process.

Study Area and Data

Regional Situation

Utopia was renamed Shiyan Utopia in 2014 from Utopia County, Utopia is located in northwestern Shiyan City, Hubei Province, upstream of the Hanjiang River, known as "the barrier of E, the gateway to Yu, the throat of Shaanxi, outside the Bureau of Shu". Northeast and Henan Province Xichuan County, southwest and Zhushan County adjacent to the west and Shaanxi Province Baihe County junction, northwest and Uyutsi County intersection, north and Shaanxi Province Shangnan County (Figure 1). It is 92km wide in the north and south, 108km long in the east and west, wide at both ends, narrow in the middle, and only 6km at the narrowest point, resembling the shape of a goldfish, with a land area of 3863km^2.

Figure 1. *Utopia Geographic Location Map*
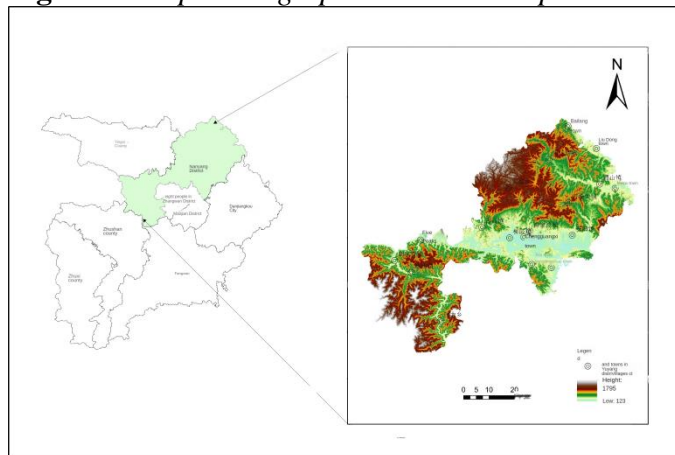
Grid Division

Considering the area of Utopia and the distribution of evaluation indexes, the grid division unit size of the study area is selected to be 500m*500m, and the Utopia is divided into 16,046 evaluation units according to the grid size of 500m*500m in ArcGIS software, and the attribute data of the evaluation indexes are assigned to each grid unit by the tool of multi-value extraction to the point in ArcGIS software, and the attribute database of the evaluation indexes is established to facilitate the subsequent evaluation study. The attribute data of evaluation indexes are assigned to each grid cell through the multi-value extraction to point tool in ArcGIS software, and the attribute database of evaluation indexes in the study area is established, which is convenient for the subsequent evaluation research.

Selection of Evaluation Factors

According to the principle of evaluation index selection, in order to select representative evaluation indexes and eliminate highly correlated evaluation indexes, therefore the correlation analysis of evaluation indexes is carried out. The thesis uses ArcGIS software to extract the attribute data of 8 evaluation indexes, and conducts Kendall correlation analysis on the 8 evaluation indexes initially selected by SPSS software respectively.The range of the Kendall correlation coefficient τ value is $[-1,1]$. When τ>0, the evaluation indicators are positively correlated with each other, when τ < 0, the evaluation indicators are negatively correlated with each other, when τ=0, it means there is no correlation, and when τ is close to 1, it means the correlation is highly correlated . The results of Kendall correlation analysis of evaluation indicators are shown in Table 1.

Table 1. *Kendall Correlation Analysis Coefficients Table*

Correlation Coefficient	Roads	Geomorphology	Tectonic (Geology)	Elevation	Slope Direction	Rainy Season	Plant Cover	Rock Group
Distance from road	1							
Landform type	0.006	1						
Distance from structure	0.052	0.001	1					
elevation	0.125	0.512	-0.022	1				
slope direction	-0.013	0.404	-0.004	0.614	1			
Distance to water system	0.080	0.06	0.054	0.038	0.011	1		
vegetation cover	0.205	0.007	0.011	0.293	-0.038	0.063	1	
Rock group type	0.063	-0.044	-0.068	0.057	-0.017	-0.12	0.157	1

The results of Kendall correlation analysis show that there is a high correlation between slope gradient and slope direction, geomorphology and slope gradient and slope direction, with correlation coefficients of 0.614, 0.512, and 0.404, respectively, which may be due to the fact that the slope gradient, slope direction, and geomorphology are all analyzed according to the elevation data by the ArcGIS software, and therefore the correlation is high. The Kendall correlation coefficients between the remaining geohazard evaluation indicators were all ≤|0.3|. Therefore, the geomorphology and slope direction indicators with high Kendall correlation coefficients were excluded.

After Kendall analysis of the indicators in Utopia, it was determined that the geohazard susceptibility evaluation index system of the dissertation finally consists of the following six indicators: ① distance from roads, ② distance from tectonics, ③ slope, ④ distance from water system, ⑤ vegetation coverage, and ⑥ rock group category. The final established evaluation index system of geologic disaster susceptibility in Utopia is shown in Figure 2.

Figure 2. *Evaluation Index System of Geologic Disaster Susceptibility in Utopia*
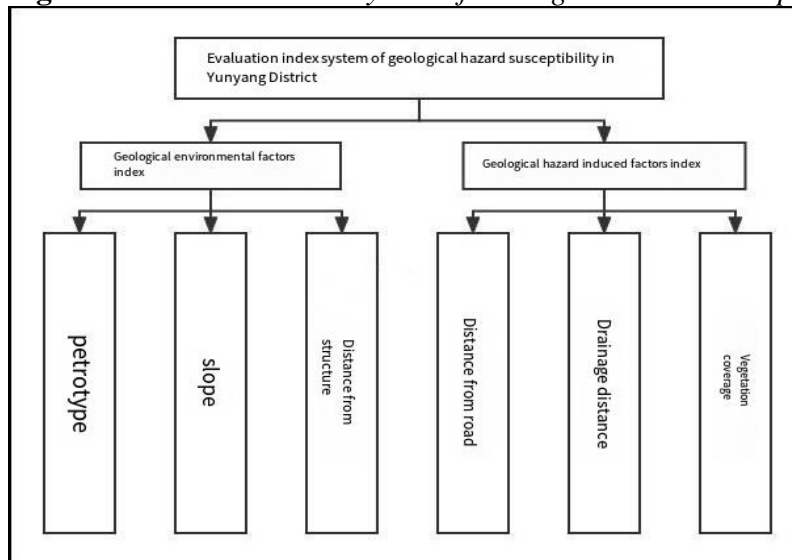
Data Processing

Evaluation system, data processing of evaluation indicator layers in ArcGIS software. The element class files of each indicator layer were converted into raster files, and then the reclassification function in the ArcGIS toolbox was used to classify each indicator according to its defined category. Subsequently, the multi-value extraction to point function was used to extract the categorized attributes of the evaluation indicators into the evaluation grid cells of the study area, and each cell had a corresponding number FID, so that the attributes of the evaluation cells had been given.

There are 892 disaster points in the study area, and the disaster points are divided into the training and validation sets of the evaluation model in the ratio of 7:3, i.e., 627 disaster points are used for training and evaluation of the model, and 265 disaster points are used for the subsequent testing of the accuracy of the model evaluation results.

The machine learning algorithm needs sample set to train the model, which consists of input indicators and output indicators, where the input indicators are the indicator attributes of the evaluation cells, and the output indicators are the results of the susceptibility partition. Considering the number of evaluation grid cells in the study area, the paper selects 627 disaster grid cells as the sample set of disaster points, and then randomly selects twice the number of grid cells as the sample set of non-disasters from the grid cell area of non-disasters, i.e., 1254 non-disasters, to form the sample set, and then according to the "Shiyan City Geological Disasters Refined Meteorological Risk Early Warning Forecast Project" project research in the partitioning area, the sample set is composed of input indicators and output indicators. The sample set is composed of 1254 non-hazardous point samples, and then the susceptibility zoning results of the sample set are extracted from the zoning results of the "Shiyan City Geological Hazard Refined Meteorological Risk Early Warning and Forecasting Project".

Methodologies

BP Neural Network

Modeling of BP Neural Networks

When solving problems, it is crucial to construct a reasonable model. In this study, we used a 3-layer neural network, with the input layer containing 6 nodes corresponding to landslide susceptibility evaluation indexes and the output layer containing 1 node. Among them, the hidden layer is 1 layer. In practice, although the number of nodes in the hidden layer can be chosen arbitrarily, we found that decreasing the number of nodes in the hidden layer increases the model output error, while increasing the number of nodes in the hidden layer reduces the model output error. However, increasing the number of hidden layer nodes leads to an increase in the number of weight matrices. Therefore, weighing the accuracy and efficiency, this study chooses a moderate number of hidden layer nodes. Through extensive debugging and training, the number of hidden layer nodes of this BP neural network is set to 15.

The parameters of the BP neural network are set as follows, the maximum number of training times is set to 1000, the learning rate is set to 0.01, and the learning accuracy is set to $1e^{-8}$, in order to achieve the desired desired value of the output results, it is necessary to repeatedly train the model until the error reaches the requirements before stopping the training. The model training process is shown in Figures 4.3, 4.4 and 4.5. Eventually, the highest model training set accuracy of the BP neural network model over the multiple training process is 94.96% as shown in Figure 3.

Figure 3. *Accuracy of BP Neural Network Training Set*
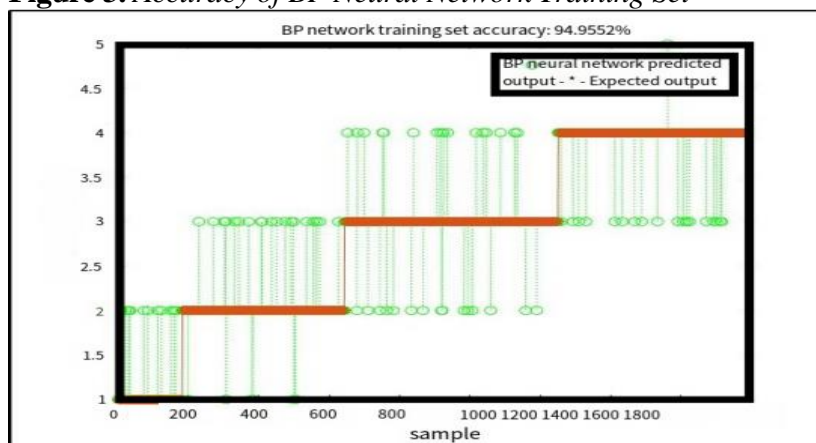

Support Vector Machine

Support Vector Machine Modeling

The paper uses support vector machines with four kinds of kernel functions as evaluation models to carry out the evaluation of geohazard susceptibility in the study area, respectively. The LN-SVM, PL-SVM, RBF-SVM, and Sigmoid-SVM

evaluation models were established by MATLAB platform and LIBSVM software package respectively. In the support vector machine evaluation model, the selection of appropriate kernel function parameter g and error penalty parameter c is crucial to the model performance of SVM.

In this paper, the K-fold cross-validation method is used to verify the training performance of the optimal parameters of the SVM model.K-fold cross-validation, that is, the data are randomly and evenly divided into K parts, of which (K-1) parts are used to build the model, and the validation is carried out in the remaining part of the data. In this paper, the value of K is chosen as 5, and the sample set is imported into the MATLAB platform, and the optimal penalty parameter c of the SVM model is sought by the K-fold cross-validation method as 6.9644, and the parameter g is 3.4822, and the optimal accuracy of cross-validation is 88.09%, as shown in Figure 4.

Figure 4. *Optimal Parameters (c, g)*
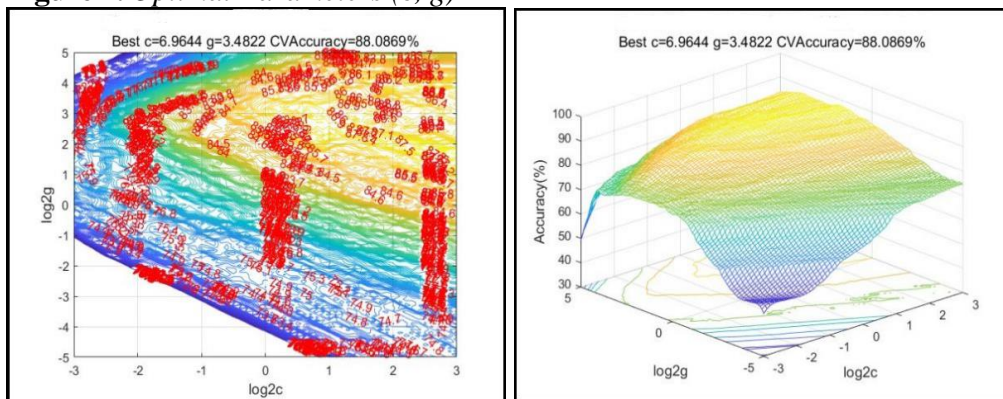
The LN-SVM, PL-SVM, RBF-SVM, Sigmoid-SVM models and the optimal parameters (c, g) are trained on the sample set to obtain the LN-SVM, PL -SVM, RBF-SVM, and Sigmoid-SVM optimal models, and the accuracy of the trained sample set with different kernel function models are 94.4507%, 90.9753%, 95.6278%, and 94.4507%, respectively, as shown in Figure 5.

Figure 5. *Training Accuracy of Sample Set of 4 Kernel Function Models*
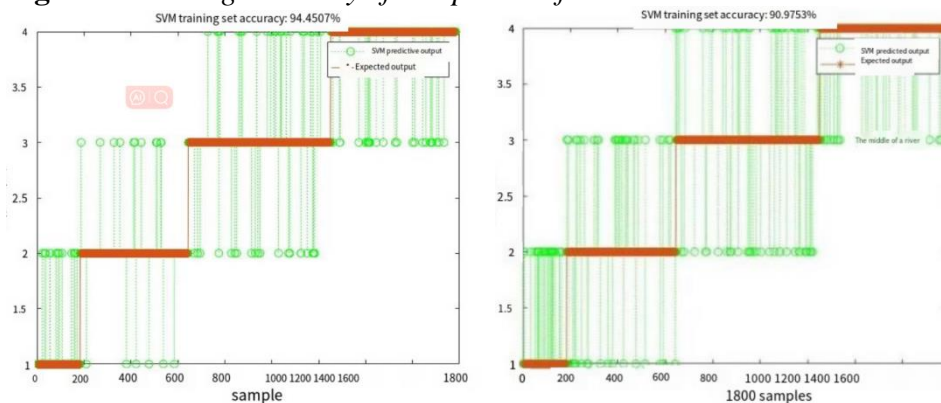
LN-SVM model PL-SVM model
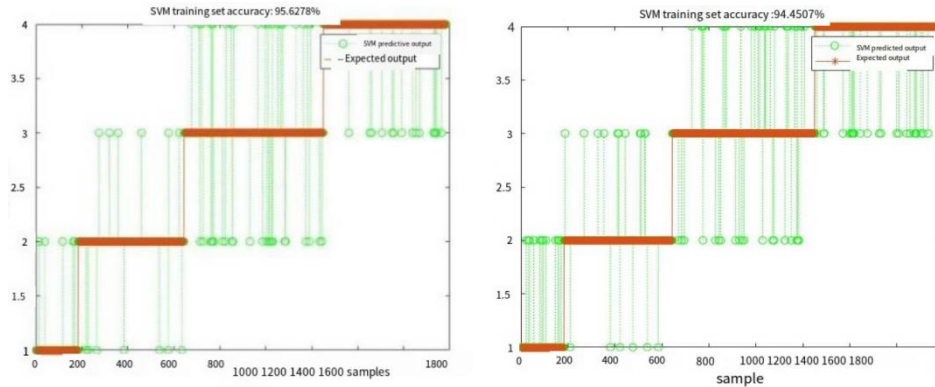
RBF-SVM model Sigmoid-SVM model

Among them, RBF-SVM model has the highest training accuracy, followed by Sigmod-SVM model and LN-SVM model, and PL-SVM model has the lowest accuracy. It can be seen that the training effect of RBF-SVM model is the best, so the RBF-SVM model was finally selected as the training model for geohazard susceptibility assessment in the study area to predict the results of susceptibility zoning in the study area.

Information Quantity Evaluation Model

Results of Single-Factor Informativeness Calculations

The grading of each evaluation factor and the distribution of disaster points in Utopia have been briefly counted above, and the information quantity of each evaluation factor was calculated according to the formula, and the information quantity of a single factor was brought into the attribute statistical table of the study area to calculate the total information quantity I_i of the evaluation grid in the study area, and subsequently, the total information quantity value was imported into ArcGIS software, and according to the method of natural breakpoints, it was classified into geohazard low susceptibility zone, medium susceptibility zone, medium high susceptibility zone and high susceptibility zone.

Results

Visualization of the Results of the Three Model Evaluations

The results of the three model evaluations were imported into the evaluation grid attributes of the study area in ArcGIS software according to the corresponding grid number for visualization and analysis, and the study area was classified into low susceptibility, medium susceptibility, medium-high susceptibility and high susceptibility according to the respective evaluation results, and the susceptibility zones of the evaluation results of the three models are shown in Figures 6-8.

Figure 6. *Evaluation Result of the Susceptibility of Information Model in Yunyang District*
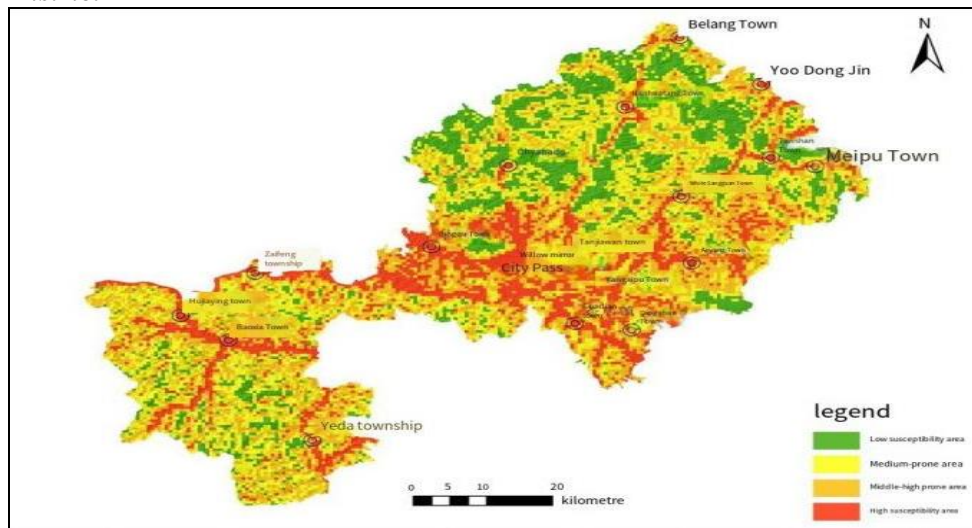

Figure 7. *Utopia BP Neural Network Model Susceptibility Evaluation Results*
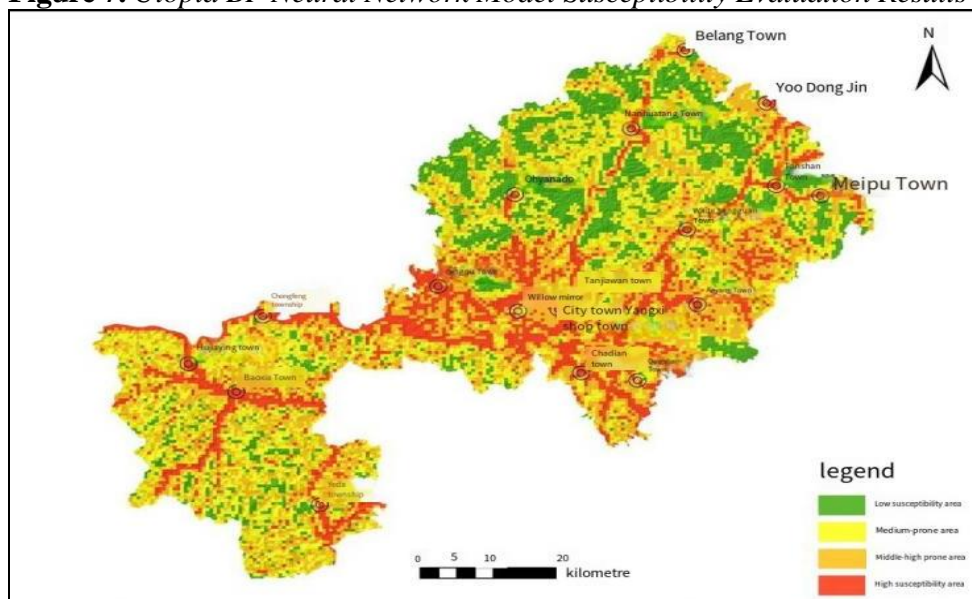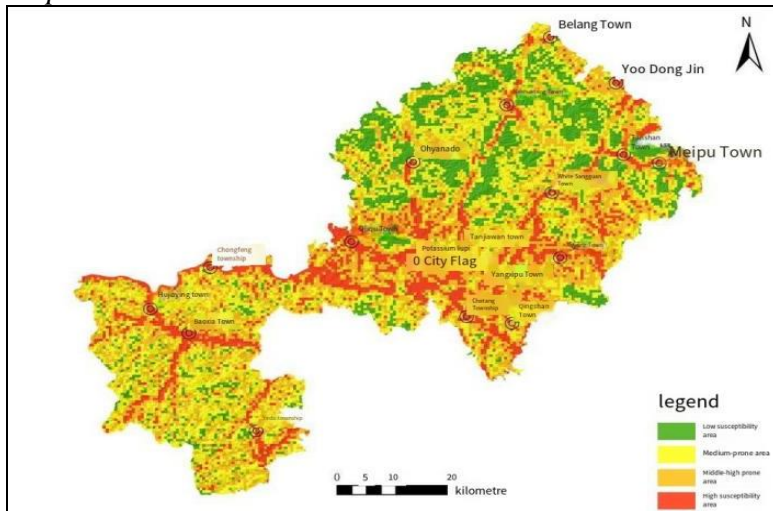
Figure 8. *Utopia Support Vector Machine Model Susceptibility Evaluation Result Map*

It can be seen that the susceptibility evaluation zoning maps of the three models are very close to each other, and the general distribution is as follows: the high susceptibility zone is distributed in the central and southwestern part of the study area, where more geohazards have already occurred; the medium and high susceptibility zones are mainly distributed in the central and eastern part of the susceptibility zone, and most of them are distributed along the perimeter of the high susceptibility zone; the medium susceptibility zones are distributed in the northern and southwestern parts of the study area, and the low susceptibility zones are distributed in the northern and northeastern parts of the study area. The medium-prone areas are located in the north and southwest of the study area, and the low-prone areas are mainly located in the north and northeast of the study area.

Comparison of the Accuracy of the Evaluation Results of the Three Models

Precision Testing

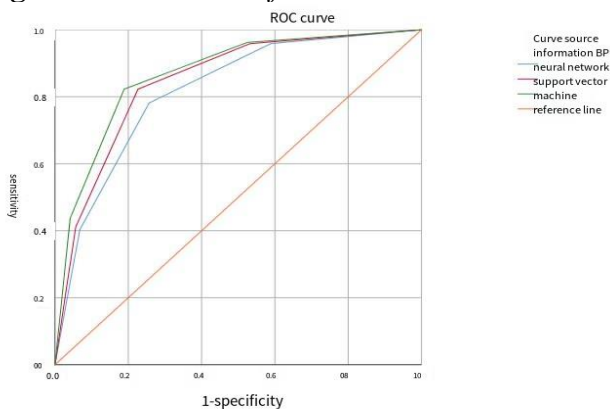**Figure 9.** *ROC Curves for the Three Evaluation Models*

Table 2. *AUC Values of the Three Evaluation Models*

Evaluation Models	AUC Value
Information quantity model	0.817
BP Neural Network Model	0.847
Support Vector Machine Model	0.868

According to Figure 9 and Table 2, it can be seen that the AUC values of the three evaluation models are relatively similar, and the AUC value of the support vector machine model is the largest, 0.868, followed by the BP neural network model, 0.847, and the last is the informative model, 0.817, so the support vector machine model has the best prediction effect in the ROC curve test.

Table 3. *Distribution of Disaster Sites*

Evaluation Models	Low susceptibility zone	Medium susceptibility zone	Medium-high susceptibility zone	High susceptibility zone
Information quantity model	25/2.8%	166/18.61%	331/37.11%	370/41.48%
BP Neural Network Model	25/2.8%	163/18.27%	338/37.89%	366/41.03%
Support Vector Machine Model	23/2.58%	162/18.16%	326/36.55%	383/42.94%

According to the Table 3, it can be seen that the distribution of disaster points in the three models is also relatively similar, in the evaluation results of the informativeness model, the distribution of disaster points in the prone area accounted for 2.8%, in the medium-prone area accounted for 18.61%, in the medium-high prone area accounted for 37.11%, and in the high prone area accounted for 41.48%; the evaluation results of the BP neural network model, the disaster points in the prone area In the evaluation results of BP neural network model, the distribution of disaster points in prone area accounts for 2.8%, in medium prone area accounts for 18.27%, in medium-high prone area accounts for 37.89%, and in high prone area accounts for 41.03%; in the evaluation results of support vector machine model, the distribution of disaster points in prone area accounts for 2.58%, in medium prone area accounts for 18.16%, in medium-high prone area accounts for 36.55%, and in high prone area accounts for 42.94%; the distribution of disaster points in the three model evaluation results in the medium-high and high susceptibility zones accounted for 78.59%, 78.92% and 79.49%, respectively. Obviously, the distribution of disaster points in the support vector machine model is the most reasonable, combined with the accuracy test results of the three models, the evaluation results of the support vector machine model are selected as the results of the geohazard susceptibility zoning in the study area.

Conclusion and Discussion

Reach a Verdict

(1) Based on the geological environment condition of Utopia, six disaster-causing influence factors, slope, rock group type, distance to water system, distance to tectonics, distance to slope and vegetation cover, were selected to construct the sample dataset for the early warning model.

(2) Based on 1881 training samples, two machine learning algorithms, BP neural network model and support vector machine model, and an informativeness evaluation model were used to carry out the evaluation study of regional geohazard susceptibility.

(3) Based on the prediction results and accuracy verification of the BP neural network algorithm model and the support vector machine algorithm model, the machine learning algorithms have excellent performance in regional geohazard susceptibility evaluation, and the prediction results are better than the traditional informativeness model.

Discussion

(1) Machine learning algorithm model in the process of model design to the visualization of prediction results, the selection of relevant parameters has a great impact on the model accuracy, and the selection of optimal parameters is one of the goals of model design.

(2) In the evaluation process, the steps of selection of evaluation indexes, grading of evaluation indexes, division of evaluation units and partitioning of susceptibility results will have an impact on the evaluation results, and there is no uniform specification in the current evaluation of regional geohazard susceptibility, and the phenomenon of strong subjectivity is common.

References

Bi R, Schleier M, Rohn J, Ehret D, Xiang W (2014) Landslide susceptibility analysis based on ArcGIS and Artificial Neural Network for a large catchment in Three Gorges region, China. *Environmental Earth Sciences* 72(6): 1925–1938.

Bragagnolo L, da Silva RV, Grzybowski JMV (2020) Artificial neural network ensembles applied to the mapping of landslide susceptibility. *Catena* 184(Jan): 104240.

Liu R, Yang X, Xu C, Wei L, Zeng X (2022) Landslide susceptibility mapping based on convolutional neural network and conventional machine learning methods. *Remote Sensing* 14(2): 321.

Moayedi H, Mehrabi M, Mosallanezhad M, Rashod ASA, Pradhan B (2019) Modification of landslide susceptibility mapping using optimized PSO-ANN technique. *Engineering with Computers* 35(3): 967–984.

Polykretis C, Ferentinou M, Chalkias C (2015) A comparative study of landslide susceptibility mapping using landslide susceptibility index and artificial neural networks in the

Krios River and Krathis River catchments (northern Peloponnesus, Greece). *Bulletin of Engineering Geology and the Environment* 74(1): 27–45.

Suryana Soma A, Kubota T, Mizuni H (2019) Optimization of causative factors using logistic regression and artificial neural network models for landslide susceptibility assessment in Ujung Loe Watershed, South Sulawesi Indonesia. *Journal of Mountain Science* 16(2): 383–401.

Tsangaratos P, Bernardos A (2014) Estimating landslide susceptibility through an artificial neural network classifier. *Natural Hazards* 74(3): 489–1516.

Valencia Ortiz JA, Martinez-Grana AM (2019) A neural network model applied to landslide susceptibility analysis (Capitanejo, Colombia). *Geomatics Natural Hazards & Risk* 9(1): 1106–1128.

Van Dao D, Jaafari A, Bayat M, Mafi-Gholami D, Qi C, Moayedi H, et al. (2020) A spatially explicit deep learning neural network model for the prediction of landslide susceptibility. *Catena* 188(May): 104451.

Experimental Analysis of CSC-type Shear Connectors Behavior under Direct Shear: Pry-Out Test (I)

By Xavier Fernando Hurtado Amézquita[*] &
Maritzabel Molina Herrera[±]

The use of steel and concrete composite sections has been recorded since the early 1950s, mainly in Europe and North America, as pioneers in the industrial production of steel elements. These systems have become popular in the world due to the efficiency of structural behavior, where steel withstands tension and concrete develops its bearing capacity in compression, being essential for the installation of stress transfer elements at the interface, called shear connectors. Recently, the use of cold-formed steel sections (CFS) has been included as a cost-effective alternative in the construction of small and medium-sized buildings. In this way, it complements concrete elements, allowing the formation of highly efficient systems, mainly in flooring systems. In this research the experimental validation of the behavior of CSC-type shear connectors is proposed, configured by Hurtado & Molina (2020), which are applicable to these CFS-concrete configurations. Pry-out tests were carried out, initially proposed by Anderson & Meinheit (2005), where the axial tensile load is applied to the steel section. This alternative experimental proposal differs from traditional push-out tests, since compressive loads can generate local bucking in steel shapes, particularly in CFS sections. The experimental results were statistically analyzed, evaluating the incidence of the compressive strength of the concrete, the thickness of the steel profile, and the spacing between connectors on the bearing capacity of the composite system. As a result of the research, the design formulation for CSC-type shear connectors in CFS-concrete composite sections is proposed.

Keywords: *composite sections, CSC-type shear connector, cold-formed steel (CFS), design formulation*

Introduction

Since the late 1950s, composite sections have been used in building construction, with the Swiss pioneering in Europe with the construction of the Nestlé building in Vevey in 1959 (Crisinel 1990). Subsequently, this system became widely known because of the advantages provided by the combination of materials, such as improved mechanical properties and efficiency. Thus, these composite systems became popular both in Europe and in the United States, the leading industrial powers of steel production.

Studs were the first elements used to transfer stresses between materials, ensuring connection and support. At that time, these elements had constructive advantages

---

[*]Assistant Professor, Department of Civil Engineering, De la Salle University, Colombia.
[±]Associate Professor, Department of Civil Engineering, National University of Colombia, Colombia.

for their installation and manufacture. Over the years, the research on different types of shear connectors was expanded, with different proposals such as channel shapes, angle shapes, perfobond rib plates, screw-type connectors, hooks, among others (Figure 1). These devices have different geometric and mechanical characteristics to transfer forces in composite systems in the most efficient way.

Figure 1. *Types of Shear Connectors in Composite Sections*
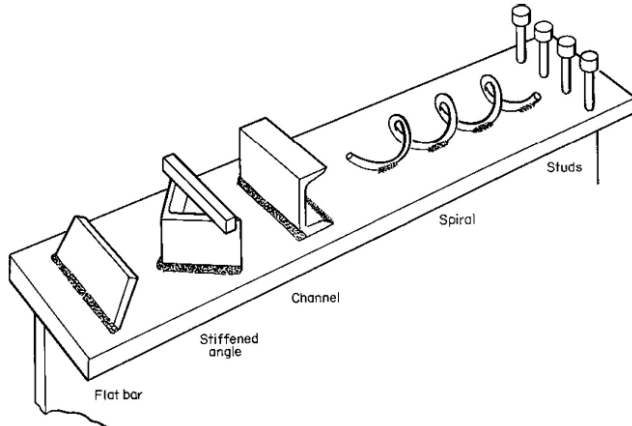
Source: Taken from Majdi et al. 2014.

Due to the technical requirements of welding and the limitations of its use in unfavorable climatic conditions, the connector fastening system is also a relevant factor in the efficiency of the construction process (Crisinel 1990). Similarly, welding has technical limitations to be applied efficiently in thin-walled elements (Figure 2).

Figure 2. *Damages in CFS Steel Plates caused by Welding Process*

Source: Erazo & Molina (2017).

Currently, the shear connectors approved in various international design codes are studs, channel shapes, perfobond rib plates, and screw-type connectors. However, it is mandatory to carry out an experimental plan to validate the bearing resistance of any other type of unregulated device. Among the experimental tests proposed for the validation of the system capacity are the direct shear tests, called *push-out test*, and the long-scale beam test. Shear tests are easier to perform than bending tests due to the size of the specimens and their maneuverability, and provide more conservative results (Crisinel 1990).

In this study, the alternative experimental pry-out test, originally designed by Anderson & Menheit (2005), is proposed. In this test, the load is applied by traction in the steel shape instead of compression, thus eliminating the possible local buckling problems generated mainly in thin-walled steel sections. In addition, this experimental arrangement is a cheaper alternative due to the geometric configuration.

In the experimental configurations tested, the capacity of CSC-type shear connectors was validated. These devices were proposed by Hurtado and Molina (2020). The incidence of the concrete strength, the thickness of the steel shapes, and the spacing of the connectors were involved in the final capacity of the composite system. As a result of the research, the load-displacement curves of the system were obtained. The statistical incidence of the mentioned variables and their relevance in a design formulation for CSC-type shear connectors involved in CFS-concrete composite sections were evaluated.

Background

Traditionally, experimental tests to study the behavior and maximum capacity of shear connectors in composite systems are full-scale beam tests and push-out shear tests, which are protocolized in Eurocode 4 and are the most commonly used methodology to obtain design formulations.

Due to the specimen dimensions of each type of test, and the complexity of the setup, the push-out test is considered the easiest to perform. The specimens are made up of two concrete slabs attached to a steel section. The axial compressive load is applied monotonically on the steel element and the stresses are transferred to the slab through the shear connectors, as shown in Figure 3.

Figure 3. *Push-out Test Setup*
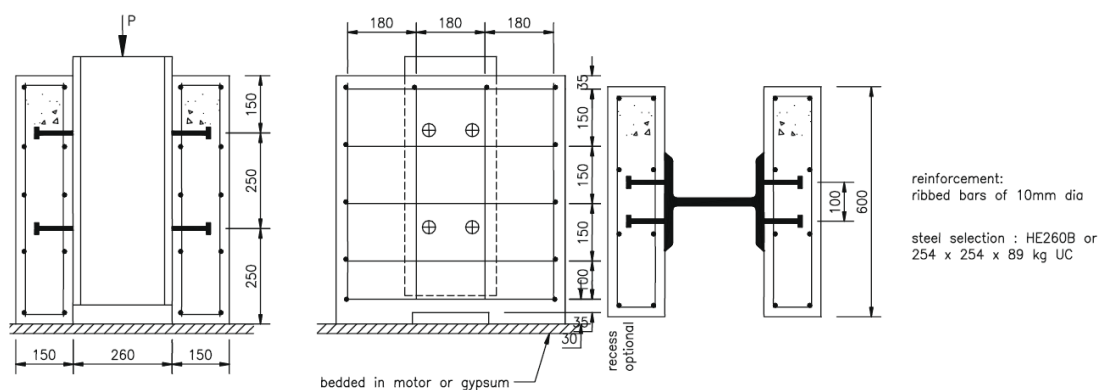
Source: Eurocode4.

Likewise, the Indian code for the design of composite sections (IS 11384-1985) proposes a different experimental setup for shear testing. The interaction is induced by two L-sections of steel and concrete joined by shear connectors at the interface. This arrangement allows loads to be applied over larger areas and specimens to be supported, as shown in the scheme presented in Figure 4.

Figure 4. *Setup of Shear Test Proposed in the Indian Design Code*
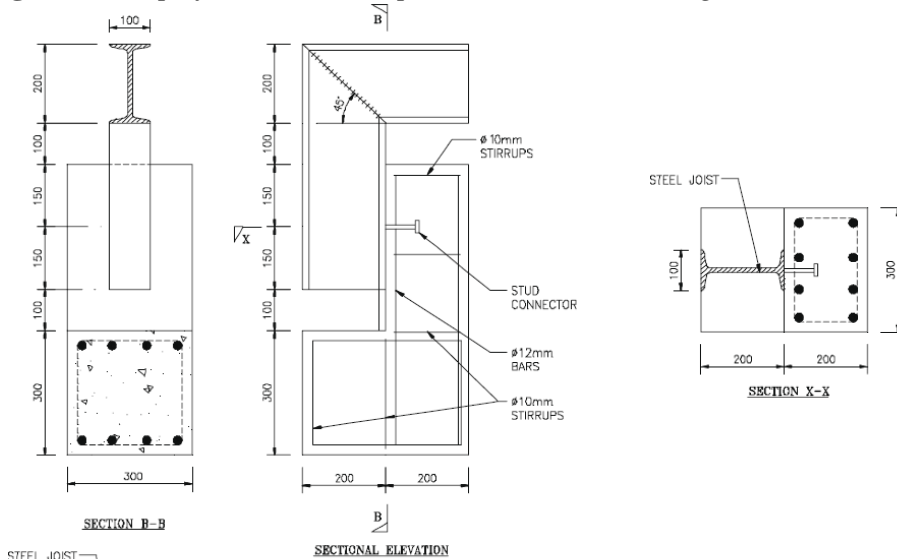
Source: IS 11384-1985.

According to the experimental test conditions, mainly in cold-formed steel sections, compressive loads have shown the induction of premature failure by local buckling in the steel plates without effectively validating the connector capacity, as presented in Lawan's (2016) research and shown in Figure 5.

Figure 5. *Failure by Local Buckling in Cold-formed Steel Sections in Push-out Test*

a)   b)
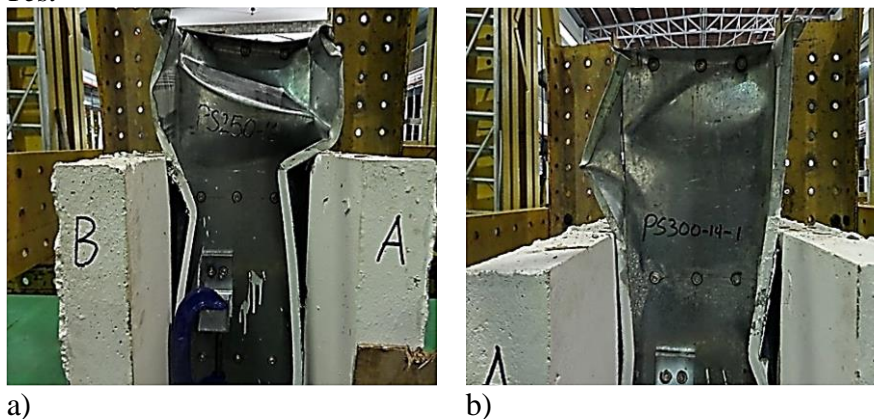
Source: Lawan et al. 2016.

Anderson & Menheit (2005) alternatively proposed the pry-out shear test, which eliminates this logistical disadvantage. The configuration of the specimens is modified from the *push-out tests* to a single concrete slab. The monotonic load is applied as traction on the steel profile, as shown in Figure 6.

Figure 6. *Setup of Alternative Pry-out Test*

a)   b)
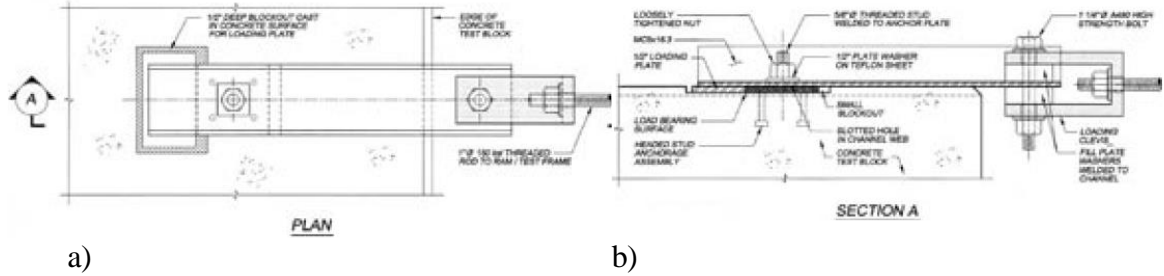
*Source:* Anderson & Menheit 2005.

Load vs. displacement curves are obtained as a result of the characterization of the behavior and capacity of the shear connectors in experimental tests. These curves make it possible to compare the performance of different configurations of the composite systems with different study parameters, such as the type of connector, the strength of the concrete, the spacing between connectors, the strength of the steel, among others (Figure 7).

Figure 7. *Load vs. Displacement Curve. a). Typical Scheme of Behavior. b) Idealization of Analytical Behavior*

a)

b)
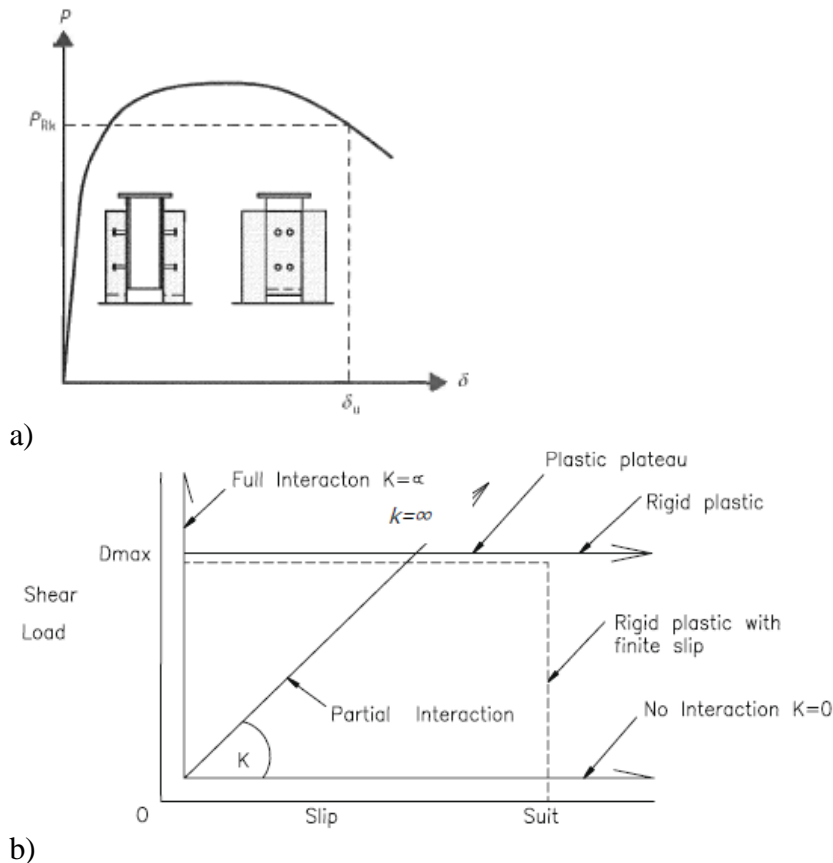
Source: a). Eurocode4 b) Johnson & Buckby 1994.

Along with experimentation, numerical simulation has become a very powerful analytical tool to achieve a good representation of computational mechanics systems, applying the finite element method (FEM), as reported by Crisinel (1990), Jeong et al. (2005), Hurtado (2007), Derlatka et al. (2019), Titoum et al. (2016), among others (Figure 8). Calibration in numerical models from material properties and constitutive models of materials, configuration of an adequate geometry, and correct simulation of support conditions are the most important factors to achieve a good representation of analytical models using specialized software. In addition, numerical models allow access to analysis results anywhere in the model.

Figure 8. *Two-dimensional Computational Model of Push-out Test a) I-type Connector Modeling Geometry b) I-type Connector Analysis Result c) Comparison of Connector Deformations in Experimental Test and I-type Connector Simulation d) Final State of Displacements Screw-type Shear Connector in Three-dimensional Numerical Model e) Final State of Displacements Screw-type Shear Connector in Experimental Specimen*

a).   b).   c).

d).   e).
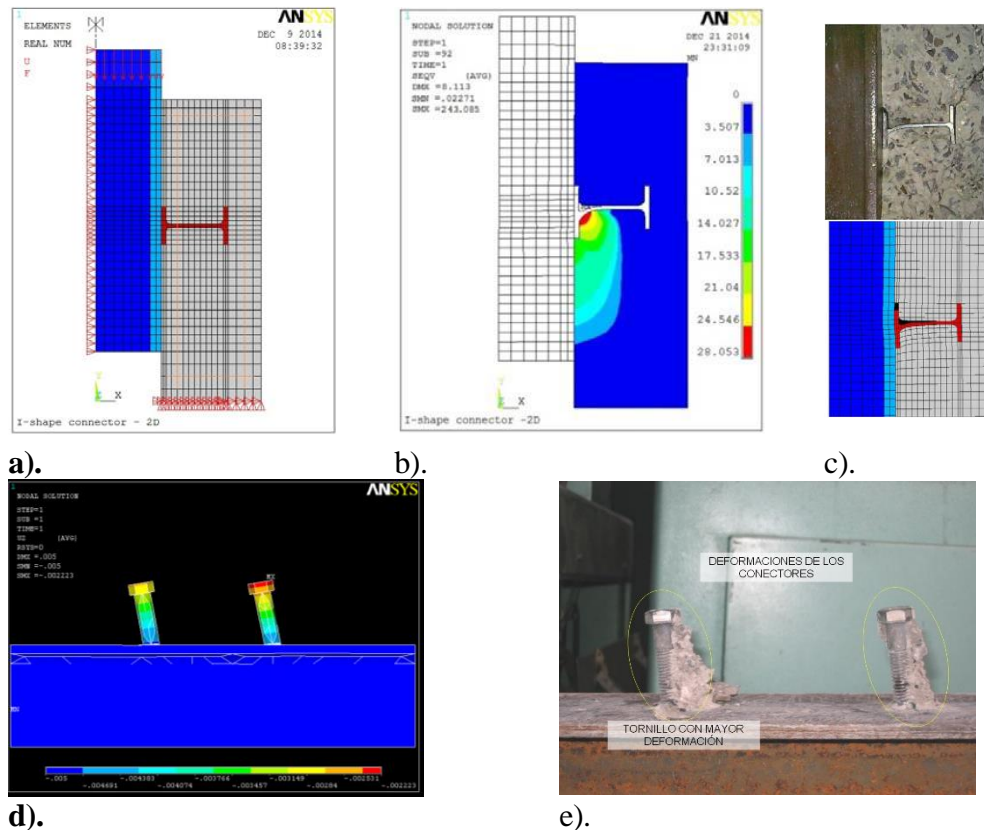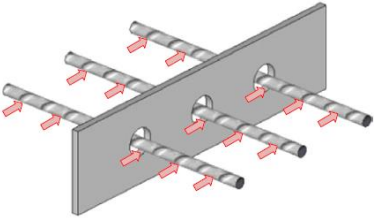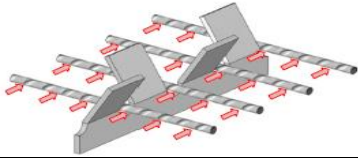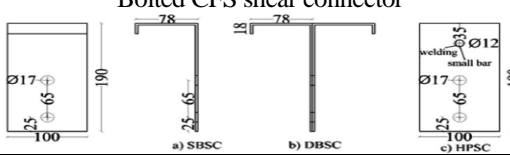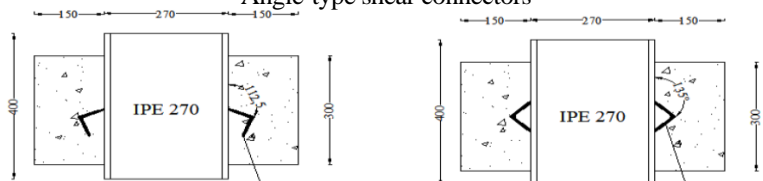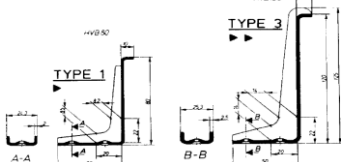
Source: a), b) and c) from Titoum et al. 2016 d) and e) from Hurtado 2007.

Through this methodology of direct shear tests, both experimental and through analysis of numerical simulation models, it has been possible to statistically correlate different parameters that directly affect the capacity of composite systems. In this way, different design expressions have been proposed to estimate the capacity of the shear connectors, without being standardized in any international design code.

Table 1 lists different design formulations for estimating the bearing capacity of different types of shear connectors that have been reported in different investigations, but have not been included in any design code for the configuration of composite sections.

Table 1. *Design Formulations for Different Types of Shear Connectors, Registered in Investigations*

Author	Design formulation	
	Perfobond rib connectors	
Oguejiofor & Hosain (1994)	$Q_{rib} = 0.59 A_{cc}\sqrt{f'_c} + 1.23 A_{tr} F_y + 2.87 n_{rib} \pi d_{rib}^2 \sqrt{f'_c}$	(1)
Oguejiofor & Hosain (1997)	$Q_{rib} = 4.50 h_{rib} t_{rib} f'_c + 0.91 A_{tr} F_y + 3.31 n_{rib} \pi d_{rib}^2 \sqrt{f'_c}$	(2)
Hosaka et al. (2000)	$Q_{hole} = 3.38 \sqrt{\dfrac{t_{rib}}{d_{rib}}} d_{rib}^2 f'_c - 39x10^3$ $22x10^3 < \sqrt{\dfrac{t_{rib}}{d_{rib}}} d_{rib}^2 f'_c < 194x10^3$	(3)
Hosaka et al. (2000)	$Q_{hole} = 1.45\left[(d_{rib}^2 - d_{tr}^2)f'_c + d_{tr}^2 F_u\right] - 26.1x10^3$ $51x10^3 < (d_{rib}^2 - d_{tr}^2)f'_c + d_{tr}^2 F_u < 488x10^3$	(4)
Sara & Bahram (2002)	$Q_{rib} = 0.747 b_{ecs} h_{ecs} \sqrt{f'_c} + 0.413 b_f L_c + 1.66 n_{rib} \pi \left(\dfrac{d_{rib}}{2}\right)^2 \sqrt{f'_c} + 0.91 A_{tr} F_y$	(5)
Medberry & Shahrooz (2002)	$Q_{slab} = 0.90 A_{tr} F_y + 0.747 b_{ecs} h_{ecs} \sqrt{f'_c} + 0.413 b_f L_c + 1.304 n_{rib} d_{rib}^2 \sqrt{f'_c}$	(6)
Verissimo et al. (2007)	$Q_{rib} = 0.404 \dfrac{h_{rib}}{b_{rib}} h_{rib} t_{rib} f'_c + 2.37 n_{rib} d_{rib}^2 \sqrt{f'_c} + 0.16 A_{cc}\sqrt{f'_c} + 31.85x10^6 \left(\dfrac{A_{tr}}{A_{cc}}\right)$	(7)
Al-Darzi et al. (2007)	$Q_{rib} = 0.762 h_{rib} t_{rib} f'_c - 7.59x10^{-4} A_{tr} F_y + 3.97 n_{rib} d_{rib}^2 f'_c + 255310$	(8)
Ahn et al. (2010) 1 connector	$Q_{rib} = 3.14 h_{rib} t_{rib} f'_c + 1.21 A_{tr} F_y + 3.79 n_{rib} \pi \left(\dfrac{d_{rib}}{2}\right)^2 \sqrt{f'_c}$	(9)
Ahn et al. (2010) 2 connectors	$Q_{rib} = 2.76 h_{rib} t_{rib} f'_c + 1.06 A_{tr} F_y + 3.32 n_{rib} \pi \left(\dfrac{d_{rib}}{2}\right)^2 \sqrt{f'_c}$	(10)
Zhao & Liu. (2012)	$Q_{hole} = 1.38 (d_{rib}^2 - d_{tr}^2) f'_c + 1.24 d_{tr}^2 F_y$	(11)

Liu et al. (2016)	$Q_{hole} = 1.85[(A_{rib} - A_{tr})f'_c + A_{tr}F_u] - 26.1x10^3$	(12)
Liu et al. (2016)	$Q_{hole} = 1.76(A_{rib} - A_{tr})f'_c + 1.58A_{tr}F_y$	(13)

Y-Type perfobond rib connector

Jung et al. (2013)	$Q_{Y.rib} = 3.428\left(\frac{d_{rib}}{2} + 2h_{rib}\right)t_{rib}f'_c + 1.213A_{tr}F_y + 1.9n_{rib}\pi\left(\frac{d_{rib}}{2}\right)^2\sqrt{f'_c} +$ $0.438m_{rib}h_{rib}s_{rib}\sqrt{f'_c}$	(14)

Bolted CFS shear connector

Tahir et al. (2019)	$Q_{con} = 4.50h_{con}t_{con}f'_c$	(15)

Angle-type shear connectors

Shariati et al. (2017) Angle 112.5°	$Q_{112.5} = 1.57\sqrt{f'_c}t_{con}^{0.35}L_{con}^{0.48}$	(16)
Shariati et al. (2017) Angle 135°	$Q_{135} = 11\sqrt{f'_c}h_{con}^{0.48}L_{con}^{-0.25}$	(17)

Bolted angle-type shear connectors

Crisinel (1990)	$Q_{con} = 0.45\sqrt{f'_cA_c} \le 0.50A_c\sqrt{f'_cE_c}$	(18)

Source: Authors.

Materials and Methods

Material Characterization

The properties of the materials were taken from their nominal values for steel elements (Table 2) and experimental validation for concrete cylinders. In this case, 3 different concrete compressive strengths were used: 14.8MPa, 22.9MPa, and 33.5MPa (Table 3).

The nominal properties of the steel elements are shown in Table 2.

Table 2. *Nominal Properties of the Steel Components in Experimental Specimens*

	CSC-Type shear connectors (ASTM A424 - Type II)	Self-drilling screws (SAE 1022)	Steel reinforcement (ASTM A706)	Steel section (ASTM A1011)
	[MPa]	[MPa]	[MPa]	[MPa]
Modulus of elasticity (Es)	200.000	200.000	200.000	200.000
Yield strength (fy)	240	205	420	350
Ultimate tensile strength (fu)	350	380	560	420

Source: Authors.

Experimental Test

In this study, experimental specimens were configured with CSC-type shear connectors and reinforcing bars. The devices were embedded in a 450mmx 300mmx 100mm concrete slab (Figure 9). In the structural configuration, N°10 self-drilling screws (4.83mm in diameter) were used for all configurations. Structural C220x80, 600mm in length, was used as steel element in various thicknesses (Table 3).

Figure 9. *Elaboration Process of the Specimens for the Pry-out Test a) Installation of Shear Connectors b) Concrete Pouring c) Assembly of the Entire System*

a)

b)

c)

Source: Authors.

The load on the system was applied monotonically as an axial traction on the steel profile; a hydraulic jack was used to apply the load. The concrete slab was fixed to the base of the Universal machine by means of a rigid system, to ensure the transfer of stresses through the shear connectors, as shown in Figure 10. The load was increased made by control of displacement.

Figure 10. *Pry-out Test Setup a) Scheme of Load Application b) Cross-section (Units in mm) c) Assembly of the Experimental Test*
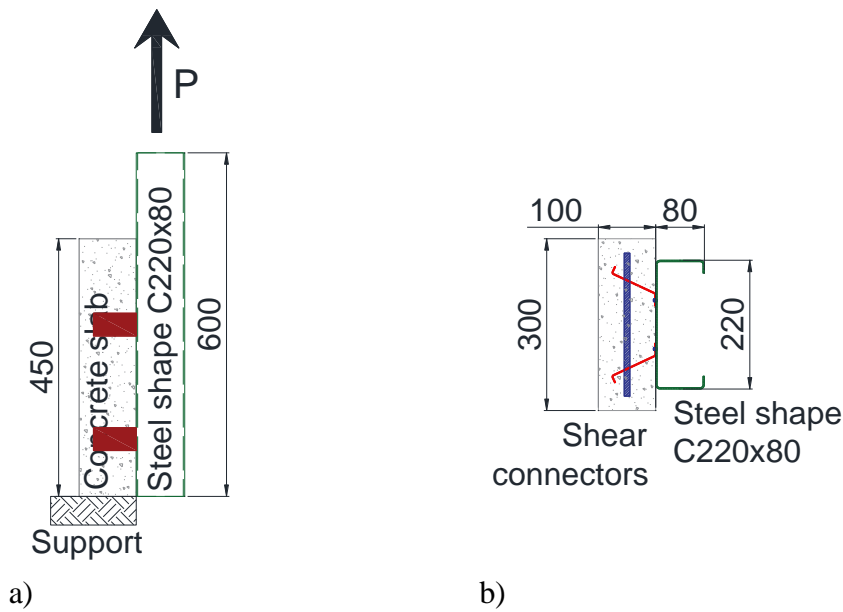
c)
Source: Authors.

Load and displacement data were recorded directly by the equipment's data acquisition system. In addition, laser measurement systems were installed to verify any differential movement between the concrete slab and the steel element. The instrumentation is shown in Figure 11.

Figure 11. *Experimental Test Instrumentation in the Pry-out Test a) Measurement of Displacements by Laser System in the Concrete Plate b) Measurement of Displacements by Laser System in Steel Profile*

a)   b)
Source: Authors.
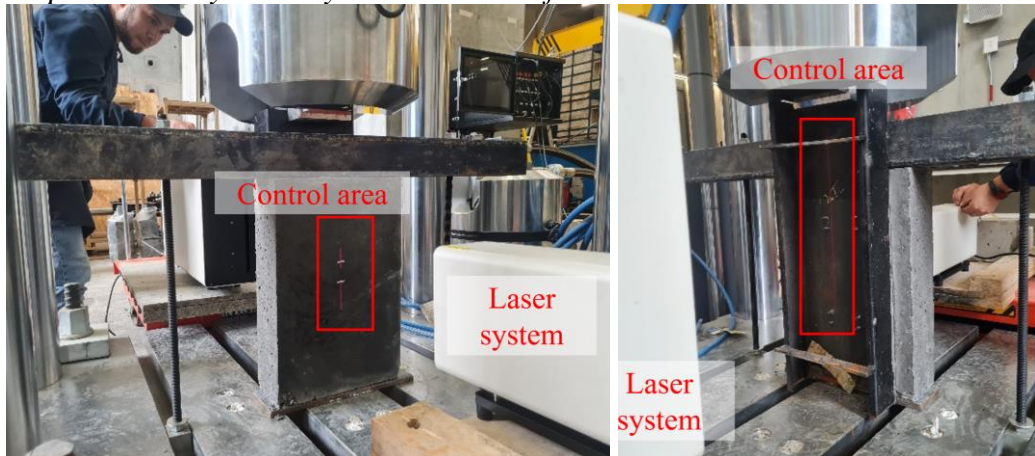
Finally, the condition of maximum displacements of the system as well as the ultimate loads and failure modes were verified. The configuration of the specimens is defined in Table 3.

Experiment Design

The Central Composite Face-Centered (CFC) design was chosen to evaluate the contribution of the study variables to the system behavior, allowing second-order fittings. In this case, the compressive strength of the concrete, the thickness of the steel profile, and the spacing between the connectors were defined as the main study parameters.

Based on the methodology, Table 3 lists the specific design points from the entire experimental matrix that were selected for testing. Figure 12 shows the graphical selection of design points. Values +1 and -1 indicate coded variables between the maximum and minimum values in the natural variables ($x1$, $x2$ and $x3$), respectively, labeled as (A), (B) and (C).

Figure 12. *Central Composite Face-centered design: Identification of Design Points*
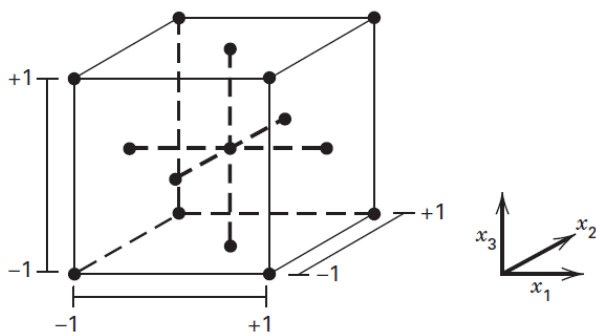
Source: Montgomery 2013.

Results and Discussion

The compressed data report from the experimental tests is shown in Table 3 and the load-displacement curves are shown in Figure 13.

Table 3. *Record of Data from Pry-out Tests*

N°	Specimen	Compressive strength of concrete (A)	Thickness of steel section (B)	Spacing between connectors (C)	Maximum force of reaction	Maximum displacement	Failure mode
		[MPa]	[mm]	[mm]	[N]	[mm]	
1	PO-2-C1@100	14.8	2.0	100	20413.99	9.07	Shear in screws
2	PO-2-C1@300	14.8	2.0	300	20880.09	7.64	Shear in screws
3	PO-2.5-C1@200	14.8	2.5	200	20241.20	5.25	Shear in screws
4	PO-3-C1@100	14.8	3.0	100	18249.52	6.65	Shear in screws
5	PO-3-C1@300	14.8	3.0	300	22705.08	6.16	Shear in screws
6	PO-2-C2@200	22.9	2.0	200	20600.25	8.34	Shear in screws
7	PO-2.5-C2@100	22.9	2.5	100	22082.57	8.39	Shear in screws

8	*PO-2.5-C2@200*	22.9	2.5	200	20500.16	5.13	Shear in screws
9	*PO-2.5-C2@300*	22.9	2.5	300	18193.47	5.28	Shear in screws
10	*PO-3-C2@200*	22.9	3.0	200	19023.60	4.30	Shear in screws
11	*PO-2-C3@100*	33.5	2.0	100	19195.98	7.93	Shear in screws
12	*PO-2-C3@300*	33.5	2.0	300	19563.39	5.82	Shear in screws
13	*PO-2.5-C3@200*	33.5	2.5	200	21536.84	4.72	Shear in screws
14	*PO-3-C3@100*	33.5	3.0	100	20134.27	5.79	Shear in screws
15	*PO-3-C3@300*	33.5	3.0	300	19110.85	3.69	Shear in screws
16	*PO-2.5-C2@200*	22.9	2.5	200	20500.16	5.13	Shear in screws

Source: Authors.

Figure 13. *Load-displacement Curves in Pry-out Test*
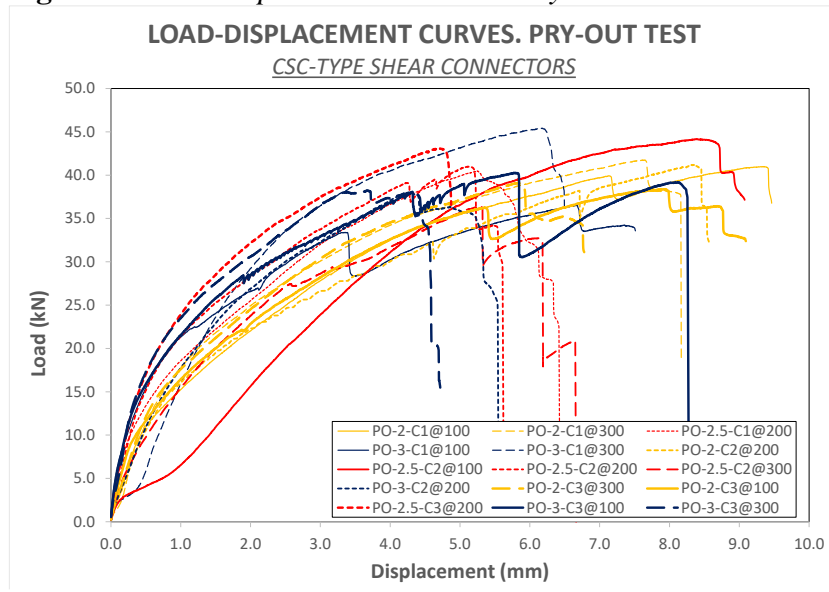
Source: Authors.

According to the results, the failure mechanism starts with the inclination of the fastening screws in the connectors. This process started earlier in the thinner steel section (Figure 14a). Subsequently, with relative displacements greater than 4mm and reaching up to 9mm, and depending on the configuration, short cracks were observed in the connectors as well as failure by shear in the screws in all the specimens (Figure 14b), with all configurations of the composite system decoupling (Figure 14d).

Figure 14. *Failure Mechanism of the Composite System. Tilted Screws after the Loading Process and Shear Failure b) Tear Detail in Shear Connectors c) Final Condition of CFS Sections (d) Final Condition of Uncoupled Specimens*

a)

b)

c)

d)

Source: Authors.

This failure condition, under service conditions in a flooring system, would imply a change in structural behavior to a non-composite system of slab and beams that must be able to withstand gravity loads.

Figure 15 shows the state of the connectors on the concrete slab, allowing their integrity within the concrete matrix to be perceived. The geometric arrangement allowed the concrete to flow under the connector and around the reinforcement while remaining completely confined. In this way, the full bearing capacity was effectively transferred across all system components.

Figure 15. *Final State of the Shear Connectors Embedded in the Concrete Slab a) General View b) Front View c) Detail of Connector and Reinforcing Bar*

a)

b)

c)
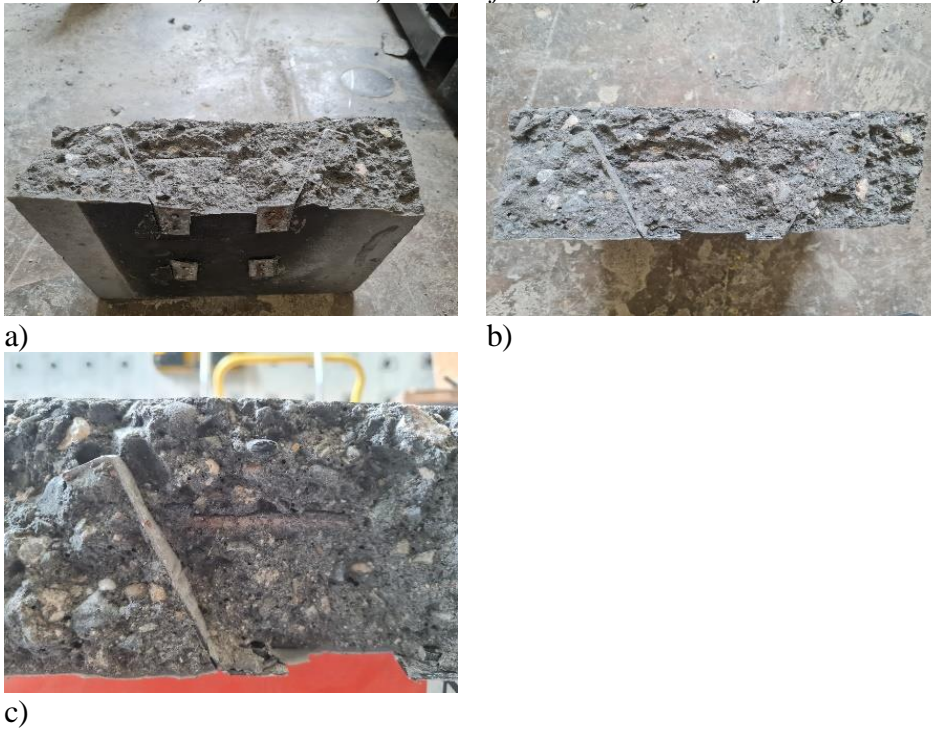
Source: Authors.

These results confirm the experimental behavior proposed by Hurtado & Molina (2020), where structural elements with thicknesses greater than 2mm presented a failure mechanism by shear in screws. At lower thicknesses, the predominant failure mode was induced by tearing of the steel plates, as shown in Figure 16.

Figure 16. *Failure Modes Presented in the Screw Shear Test a) Failure due to Screw Shear b) Failure due to Screw Tilting and Plate Separation c) Failure due to Tension on the Net Section in Plate*

a)   b)   c)
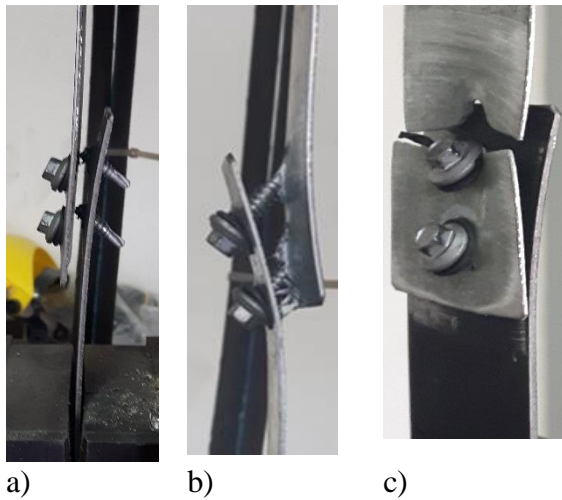
Source: Authors.

As shown in Figure 17, additional transverse cracks were likely in specimens with lower compressive strength concrete. This confirms the effectiveness of the geometric and mechanical configuration of the connector. Thus, the inclusion of the reinforcing bar guarantees the dispersion of the cracks induced by the axial load.
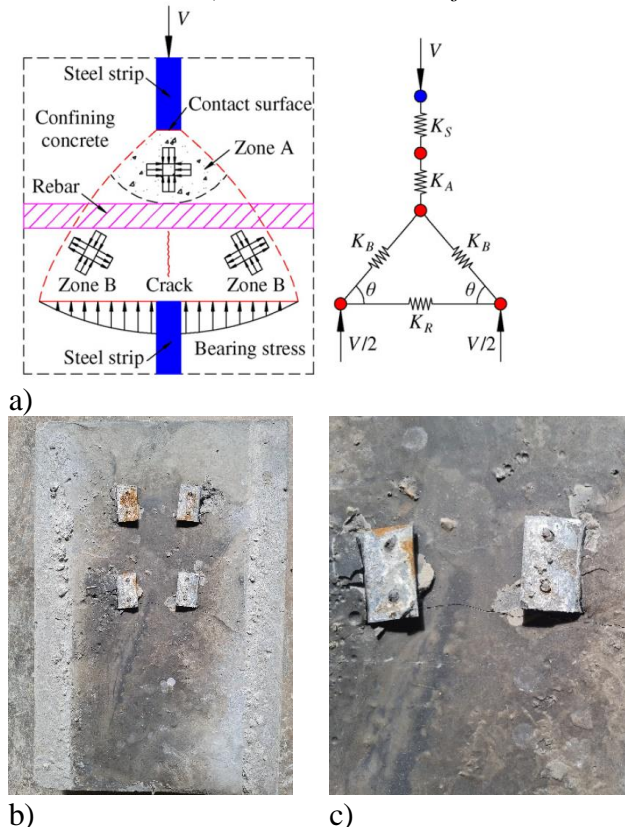
Figure 17. *Shear Transfer Mechanism Including Reinforcing Bar a) Theoretical Idealization of the Mechanism b) General View Induction of Transverse Cracks in Concrete Plate c) Detail Induction of Transverse Cracks in Concrete Plate*

a)

b)   c)

Source: a) Taken from Liu et al. 2015 b) and c) Authors.

This failure condition aims to predict that, under the same conditions of this research, the compressive strength of the concrete is not relevant in the maximum capacity of the composite system, where the failure is governed by shear in screws.

Statistical Response

The statistical response is approached from the behavior of the maximum reaction force of the system and the maximum displacement reached, evaluating the incidence of the variables involved in the study on the performance and maximum capacity of the system: (A) compressive strength of concrete, (B) thickness of the steel profile and (C) spacing between connectors (Table 3).

Shear in self-drilling screws was the failure mode that determined the damage in all specimens. Therefore, there were no statistically significant differences among the experimental arrangements tested. Figure 18 shows the statistical confidence intervals for the maximum load reaction with a 95% probability of failure for both the concrete compressive strength (Figure 18a), the steel shape thickness (Figure 18b), and the spacing between connectors (Figure 18c), where the overlapping response values show statistical equality.

Figure 18. *Confidence Interval for Maximum Load Reaction with 95% Probability a) Compressive Strength of Concrete (b) Thickness of the Steel Shape c) Spacing between Connectors d) Interaction Plot for Maximum Force Reaction Response*
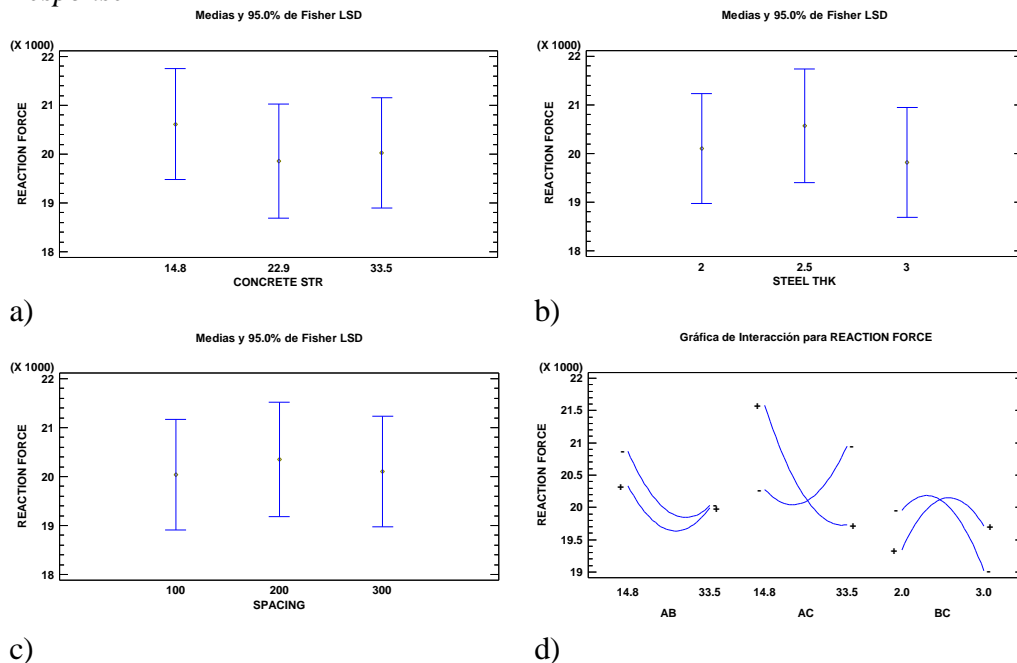
Source: Authors.

Figure 18d shows the interaction plot for all the parameters, where the intersection implies the simultaneous work of all the variables under the proposed configurations.

On the other hand, to evaluate the maximum displacements, the confidence intervals of the statistical response allow to appreciate significant differences for all the variables studied. It has been concluded that the failure condition presents sensitive deformations depending on the different arrangements of the composite systems, with values exceeding 6mm (Figure 19).

Figure 19. *Confidence Interval for Displacement Load Reaction with 95% Probability a) Compressive Strength of Concrete (b) Thickness of the Steel Shape c) Spacing between Connectors d) Interaction Plot for Maximum Force Reaction Response*
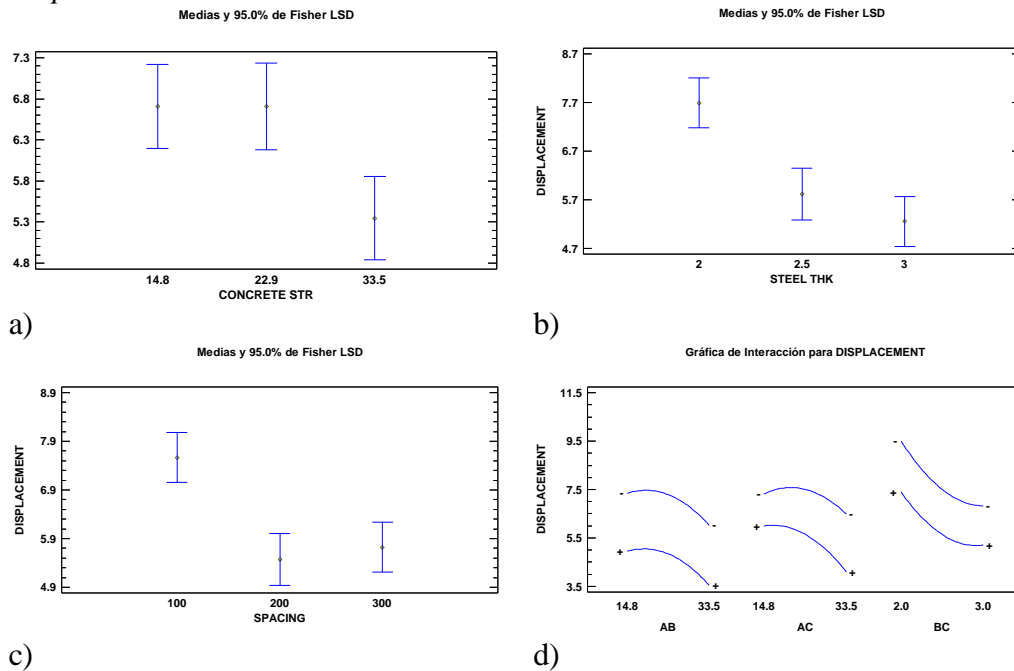

Source: Authors.

Unlike the maximum reaction response, the displacement condition does not show the interaction of the variables, which indicates that changing the values of each one of them separately affects the final displacement condition (Figure 19d).

Parametric Analysis

The parametric analysis made it possible to determine the incidence of the studied variables in the final states of behavior of the composite systems, in particular the maximum reaction loads and the maximum displacements.

Effect of the Compressive Strength of the Concrete

In some specimens, cracks appeared in the concrete slabs as part of the simultaneous failure mechanism of the composite system without total failure of the concrete. As shown in Figure 18a and Figure 19a, this variable is not considered statistically significant in the maximum load capacity of the composite systems, but it does make a difference in the maximum displacement condition. The lower strengths show larger displacements according to the stiffness of the materials.

Effect of Steel Profile Thickness

Similarly to concrete, the thickness of the steel section only affects the stiffness condition of the system, implying greater displacements in elements with

lower thicknesses, as can be seen in Figure 18b and Figure 19b. The steel profiles did not show any local or global damage in any of the configurations tested.

Effect of Connector Spacing

The spacing between connectors marked a strong difference in the maximum relative displacements between the materials, which were greater in the specimens with smaller spacing (Figure 19c). This situation indicates that smaller separations give the system greater ductility before failure. There is no statistically significant difference regarding the maximum loads (Figure 18c).

Design Formulation

According to the behavior of the studied composite systems, the design expression of CSC-type shear connectors (19) is proposed for failures in the fastening system due to shear in the screws without major effect on the other components of the system:

$$Q_n = 13000 \cdot \alpha \cdot f'^{0.20}_c \cdot t^{0.20}_{st} \leq 4 \cdot A_{sc} \cdot F_u \qquad (19)$$

The first part of the equation is related to concrete fracture failure, adjusted from the simulation results of Hurtado and Molina (2021). α is an experimental validation parameter, taken as 1.0 for the graph in Figure 20.

Table 4 shows several cases of estimation of the maximum loads of the composite system based on the proposed design equation. It also includes the ratio of the maximum experimental load to the estimated load, with emphasis on the proposal for the No.10-screws that were tested. It can be seen that the experimental load is about 20% higher than the estimated load.

Table 4. *Estimated Failure Loads for Shear in Self-drilling Screws from the Proposed Design Equation*

N°	Specimen	Maximum experimental reaction force	Nominal failure load for N°10-Screws		Nominal failure load for N°12-Screws		Nominal failure load for N°14-Screws	
		[N]	[N]		[N]		[N]	
1	PO-2-C1@100	20413.99	**16710.10**	**1.22**	20348.82	1.00	24345.68	0.84
2	PO-2-C1@300	20880.09	**16710.10**	**1.25**	20348.82	1.03	24345.68	0.86
3	PO-2.5-C1@200	20241.20	**16710.10**	**1.21**	20348.82	0.99	24345.68	0.83
4	PO-3-C1@100	18249.52	**16710.10**	**1.09**	20348.82	0.90	24345.68	0.75
5	PO-3-C1@300	22705.08	**16710.10**	**1.36**	20348.82	1.12	24345.68	0.93
6	PO-2-C2@200	20600.25	**16710.10**	**1.23**	20348.82	1.01	24345.68	0.85
7	PO-2.5-C2@100	22082.57	**16710.10**	**1.32**	20348.82	1.09	24345.68	0.91
8	PO-2.5-C2@200	20500.16	**16710.10**	**1.23**	20348.82	1.01	24345.68	0.84

9	*PO-2.5-C2@300*	18193.47	**16710.10**	**1.09**	20348.82	0.89	24345.68	0.75
10	*PO-3-C2@200*	19023.60	**16710.10**	**1.14**	20348.82	0.93	24345.68	0.78
11	*PO-2-C3@100*	19195.98	**16710.10**	**1.15**	20348.82	0.94	24345.68	0.79
12	*PO-2-C3@300*	19563.39	**16710.10**	**1.17**	20348.82	0.96	24345.68	0.80
13	*PO-2.5-C3@200*	21536.84	**16710.10**	**1.29**	20348.82	1.06	24345.68	0.88
14	*PO-3-C3@100*	20134.27	**16710.10**	**1.20**	20348.82	0.99	24345.68	0.83
15	*PO-3-C3@300*	19110.85	**16710.10**	**1.14**	20348.82	0.94	24345.68	0.78
16	*PO-2.5-C2@200*	20500.16	**16710.10**	**1.23**	20348.82	1.01	24345.68	0.84

Source: Authors.

Similarly, Figure 20 shows the behavior of the experimental response versus the estimated capacities for various diameters of self-drilling screws used as a fastening system for CSC-type shear connectors.

Figure 20. *Estimation Loads Based on Design Equation Proposed for Different Configurations*
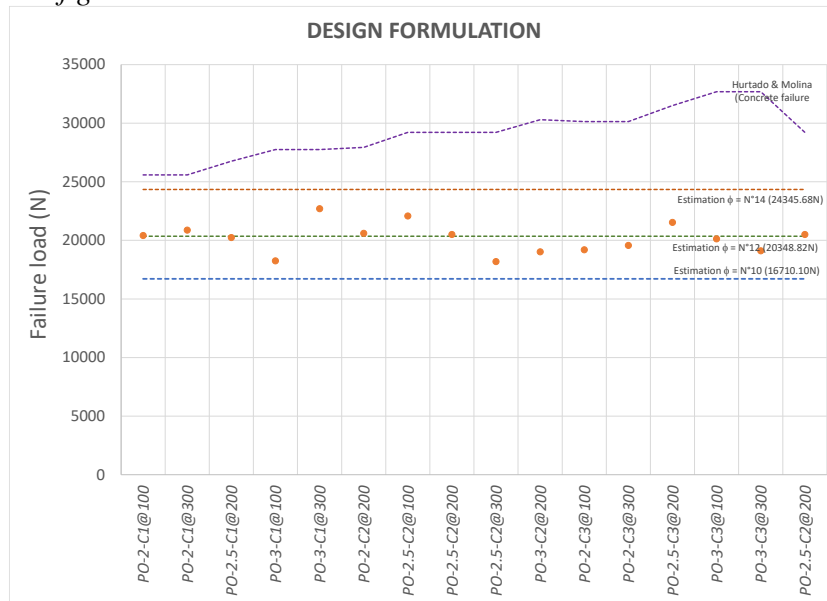
Source: Authors.

Conclusions

The pry-out test methodology for the evaluation of the capacity of composite systems has proven to be a reliable experimental alternative, particularly for cold-formed steel sections (CFS), where the effect of local buckling potential, which occurs in traditional push-out tests due to compressive load, is mitigated. This alternative experimental test can even be extrapolated to composite section configurations using hot-rolled sections (HRS) with greater plate thicknesses.

The experimental validation of the CFS-Concrete composite system, using CSC-type shear connectors, under direct shear loads, allowed the evaluation of the

working conditions of the system and its failure mechanism. This mechanism started as rotation in the self-drilling screws as fastening elements and a limited tear in the connector plate. In a similar way, specimens with lower resistances showed cracks in the concrete slab. Finally, in all the configurations tested, the screws were cut without affecting the steel profile, thus decoupling the composite system, but without loss of the integrity of the elements.

Although the experimental parameters validated in this research were not statistically different for the maximum reaction loads, it was possible to find differences in the ductility conditions of the system. This meant greater relative displacements with lower concrete resistances, lower steel profile thicknesses, and smaller spacings, reaching values greater than 6mm, as the limit of Eurocode4 for ductile shear connectors.

Finally, the design expression of CSC-type shear connectors is proposed, to be used in the design of CFS-concrete composite systems, where the failure is projected by shear in the self-drilling screws as the fastening mechanism.

References

Ahn JH, Lee CG, Won JH, Kim SH (2010) Shear resistance of the perfobond-rib shear connector depending on concrete strength and rib arrangement. *Journal Constructional of Steel Research* 66(10): 295–307.

Al-Darzi SYK, Chen AR, Liu YQ (2007) finite element simulation and parametric studies of perfobond rib connector. *American Journal of Applied Science* 4(3): 122–127.

Anderson N, Meinheit D (2000) Design criteria for headed studs groups in shear. *PCI Journal* 45(5): 46–75.

Anderson N, Meinheit D (2005) Pry-out capacity of cast-in headed studs anchors. *PCI Journal* 50(2): 90–112.

Crisinel M (1990) Partial-interaction analysis of composite beams with profiled sheeting and non-welded shear. *Journal of Constructional Steel Research* 15(1–2): 65–98.

Derlatka A, Lacki P, Nawrot J, Winoviecka J (2019) Numerical and experimental test of steel concrete composite beam with the connector made of top-hat profile. *Composite Structures* 211(Mar): 244–253.

Erazo L, Molina M (2017) *Comportamiento de conectores de cortante tipo tornillo en secciones compuestas con lámina colaborante.* (Behavior of screw-type shear connectors in composite sections with composite shell). Thesis of master's degree. Universidad Nacional de Colombia.

European Committee Standardization (2004) *Eurocode 4: Design of composite steel and concrete structures.*

Hosaka T, Mitsuki K, Hiragi H, Ushijima Y, Tachibana Y, Wantabe H (2000) An experimental study on shear characteristics of perfobond strip and its rational strength. *Journal of Structural Engineering JSCE* 46A: 1593–1604.

Hurtado X (2007) *Comportamiento de conectores de cortante tipo tornillo de resistencia grado 2 (dos) para un sistema de sección compuesta con concreto de 21MPa ante solicitación de corte directo.* (Behavior of grade 2 (two) strength screw-type shear connectors for a composite section system with 21 MPa concrete under direct shear loading). Thesis of master's degree. Universidad Nacional de Colombia.

Hurtado X, Molina M (2020) Alternative fastening mechanism for shear connectors with cold-formed steel shapes involved in composite sections. *Athens Journal of Technology and Engineering* 7(2): 133–156.

Hurtado X, Molina M (2020) Geometrical and mechanical optimization of shear connectors for CFS-concrete composite systems. In *The 2020 Structures Congress*, 25–28.

Hurtado X, Molina M (2021) Behavior of CSC-type shear connectors under pry-out shear test: analytical study. *Materials Science Forum* 1046(Sep): 45–58.

Indian Standards Institution. IS 11384-1985 (1986) *Indian standard code of practice for composite construction in structural steel and concrete*.

Jeong YJ, Kim HY, Kim SH (2005) Partial-interaction analysis with push-out test. *Journal of Constructional Steel Research* 61(9): 1318–1331.

Johnson RP, Buckby RJ (1994) *Composite structures of steel and concrete*. Oxford (England): Blackwell Scientific Publications.

Jung CH, Kim SH, Choi KT, Park SJ, Park SM (2013) Experimental shear resistance evaluation of Y-type perfobond rib shear connector. *Journal of Constructional Steel Research* 82(Mar): 1–18.

Lawan M, Tahir M (2015) Strength capacity of bolted shear connectors with cold-formed steel section integrated as composite beam in self-compacting concrete. *Jurnal Teknologi* 77(16): 105–112.

Lawan M, Tahir M, Osman H (2015) Composite construction of cold-formed steel (CFS) section with high strength bolted shear connector. *Jurnal Teknologi* 77(16): 171–179.

Lawan M, Tahir M, Ngian S, Sulaiman A (2015) Structural performance of cold-formed steel section in composite structures: A review. *Jurnal Teknologi* 74(4): 65–175.

Lawan M, Tahir M, Hosseinpour E (2016) Feasibility of using bolted shear connector with cold-formed steel in composite construction. *Jurnal Teknologi* 78(6–12): 7–13.

Lawan M, Tahir M, Mirza J (2016) Bolted shear connectors performance in self-compacting concrete integrated with cold-formed steel section. *Latin American Journal of Solids and Structures* 13(4): 731–749.

Liu Y, Zheng S, Yoda T Lin W (2016) Parametric study on shear capacity of circular-hole and long-hole perfobond shear connector. *Journal of Constructional Steel Research* 117(Feb): 64–80.

Majdi Y, Hsu C, Zarei M (2014) Finite element analysis of new composite floors having cold-formed steel and concrete slab. *Engineering Structures* 77(Sep): 65–83.

Majdi Y, Hsu C, Zarei M (2014) Finite element modeling of new composite floors having cold-formed steel and concrete slab. In *International Specialty Conference on Recent Research and Developments in Cold-Formed Steel Design and Construction*, 463–477.

Medberry SB, Shahrooz BM (2002) Perfobond shear connector for composite construction. *Engineering Journal AISC* 39(1): 2–12.

Oguejiofor EC, Hosain MU (1994) A parametric study of perfobond rib shear connectors. *Canadian Journal of Civil Engineering* 21(4): 614–625.

Oguejiofor EC, Hosain MU (1997) Numerical analysis of push-out specimenes with perfobond rib connectors. *Computers & Structures* 64(4): 617–624.

Sara BM, Bahram MS (2002) Perfobond shear connectors for composite construction. *Engineering Journal, First Quarter* 39(1): 2–12.

Shariati M, Khorramian K, Maleki S, Jalali A, Tahir MM (2017) Numerical analysis of tilted angle shear connectors in steel-concrete composite systems. *Steel and Composite Structures* 23(1): 67–85.

Tahir M, Saggaff A, Azimi M, Lawan M (2016) Impact of bolted shear connector spacing in composite beam incorporating cold formed steel of channel lipped section. *IIOAB Journal* 7(May): 441–445.

Tahir MM, Bamaga SO, Tan CS, Shek PN, Aghlara R (2019) Push-out test on three innovative shear connectors for composite cold-formed steel concrete beams. *Construction and Building Materials* 223(Oct): 288–298.

Tahir M, Bamaga S, Ngian S, Mohamad S, Sulaiman A, Aghlara R (2019) Structural behaviour of cold-formed steel of double C-lipped channel sections integrated with concrete slabs as composite beams. *Latin American Journal of Solids and Structures* 16(5): 1–15.

Titoum M, Mazoz A, Benanane A, Ouinas D (2016) Experimental study and finite element modelling of push-out test on a new shear connector of I-shape. *Advanced Steel Construction* 12(4): 487–506.

Verissimo GS (2007) *Development of a shear connector plate gear for composite structures of steel and concrete and study their behavior* (In Portuguese). Thesis of PhD's degree. Universidad Federal de Minas Gerais Belo Horizonte.

Zhao C, Liu YQ (2012) Experimental study of shear capacity of perfobond connector. *Journal of Engineering Mechanics* 29(12): 349–354.